



Studying the Wear Characteristics of Aluminium Alloys (Al2024 and Al7075) at Different Wear Conditions

A Thesis

Submitted to the Council of the Erbil Technical Engineering College at Erbil Polytechnic University in Partial Fulfillment of the Requirements for the Degree of Master of Science in Mechanical and Energy Engineering.

By:

Karmand Abubakr Ahmed

B.Sc. in Refrigeration and Air -Conditioning Engineering Techniques. 2014

Supervised by:


Dr. Dlair O. Ramadan

ERBIL-KURDISTAN

March-2023

DECLARATION

I declare that the master thesis entitled: **“Studying the Wear Characteristics of Aluminium Alloys (Al2024 and Al7075) at Different Wear Conditions”** is my own original work, and hereby I certify that unless stated, all work contained within this thesis is my own independent research and has not been submitted for the award of any other degree at any institution, except where due acknowledgement is made in the text.

Signature: 

Student Name: Karmand Abubakr Ahmed

Date: 29/3/2023

LINGUISTIC REVIEW

I confirm that I have reviewed the thesis titled (**Studying the Wear Characteristics of Aluminium Alloys (Al2024 and Al7075) at Different Wear Conditions**) from the English linguistic point of view, and I can confirm that it is free of grammatical and spelling errors.

Signature:



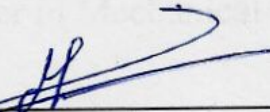
Name of Reviewer: Dilovan Sayfuddin Ghafoory

Date: 15/12/2022

Email Address: dilovan.ghafoory@su.edu.krd

SUPERVISOR CERTIFICATE

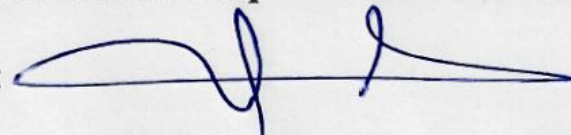
This thesis has been written under my supervision and has been submitted for the award of the degree of Master of Science in Mechanical and Energy Engineering with my approval as a supervisor.


Signature

Dr. Dlair O. Ramadan
Name

29/3/2023
Date

I confirm that all the requirements have been fulfilled.

Signature: 

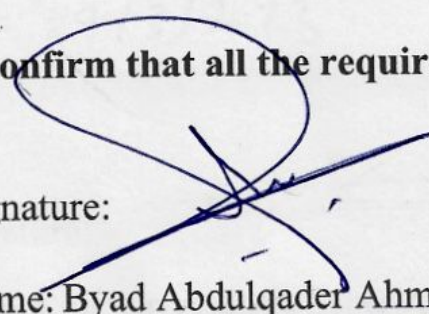
Name: Asst. Prof. Dr. Ahmed Mohammed Adham

Head of Mechanical and Energy Engineering Department

Date: 2/4/2023



I confirm that all the requirements have been fulfilled.

Signature: 

Name: Byad Abdulqader Ahmed

Postgraduate Office

Date: 4-4-2023

EXAMINING COMMITTEE CERTIFICATION

We certify that we have read this thesis entitled “**Studying the Wear Characteristics of Aluminium Alloys (Al2024 and Al7075) at Different Wear Conditions**” and as an examining committee, examined the student (Karmand Abubakr Ahmed) in its content and what related to it. We approve that it meets the standards of a thesis for the degree of Master in Mechanical and Energy Engineering.

Signature:

Name: Asst. Prof. Dr. Mohammedtaher M. Mulapeer
Member

Date:

9/3/2023

Signature:

Name: Asst. Prof. Dr. Younis Khalid Khdir
Member

Date:

29/3/2023

Signature:

Name: Dr. Dlair O. Ramadan
Supervisor

Date:

29/3/2023

Signature:

Name: Asst. Prof. Dr. Rzgar M. Abdulrahman
Chairman

Date:

29/3/2023

Signature:

Name: Prof. Dr. Ayad Z. Saber Agha
Dean of Erbil Technical Engineering College

Date:

4-4-2023

DEDICATION

First and foremost, I am dedicating this thesis to my father, who passed away 19 years ago. Although he is no longer in this world, but his memories continue to regulate my life. To my mom who loves me unconditionally and standing with me in all of my happiness and sadness moments, thanks for directing me on to the right path continuously, you have been such an inspiration to me, I couldn't do anything without you. To my dear wife, brothers, sisters and friends. Thank you, my love for you all can never be quantified. God bless you.

ACKNOWLEDGMENT

In the Name of Allah, the Most Compassionate the Most Merciful, all praise be to Allah, the Lord of the worlds.

My wholehearted thanks also go to my supervisor, Dr. Dlair O. Ramadan for his contribution, guidance, and advice, I can never pay you back for all the assistance you have done to me. Thank you for your help and support. I will be thankful to you forever. Thanks for Dr. Dler Abdullah Ahmed, at Mechanical and metallurgy department in Erbil Technical College, I am grateful for his support, and I value the insights and guidance he provides.

Next, I would like to convey my special thanks to the head of Mechanical and Energy Engineering Department and all staffs of these Department, for their kind assistant and supports. Without their kind cooperation, this study may not be completed on time. I would also like to thank the Erbil Polytechnic University, they give me the opportunity to study my Master.

I also would like to express my sincere gratitude and appreciation to my colleagues, who have given information and access to knowledge bases that have helped me greatly and they worked hard with me from the beginning of the present thesis until the completion.

ABSTRACT

In this study, a high temperature tribometer machine of pin-on-disc was designed and manufactured to examine the wear characteristics of 2024 and 7075 aluminium alloys at different wear conditions such as temperature, load, and sliding distance. The wear experiments were carried out in a dry sliding condition at temperatures ranging from 25 to 225 °C, loads of 10, 20, and 30 *N*, and sliding distances of 1570, 2356, and 3141 *m*, with constant sliding speed of 2.6 m/s throughout the testing. The results showed that when the temperature increases, the wear due to volume loss also increases. An increase in sliding distance and load increases the wear. The Microscopic analysis and Scanning Electron Microscope (SEM) of the specimens reveals that wear traces are mostly abrasive, with just small traces of adhesive wear visibility. Furthermore, the wear process switched from mild into delamination and subsequently to severe metal wear as the load and temperature continued to increase. Because of the softening impacts of the high operating temperature, the wear mechanism takes the form of massive removal of material in a sliding direction. Due to the higher hardness of Al7075, it has higher wear resistance and lower wear (volume loss) compared to Al2024.

TABLE OF CONTENTS

DEDICATION	V
ACKNOWLEDGMENT.....	VI
ABSTRACT	VII
LIST OF FIGURES.....	X
LIST OF TABLES	XIV
LIST OF ABBREVIATIONS AND SYMBOLS	XV
CHAPTER ONE	1
INTRODUCTION.....	1
1.1. INTRODUCTION	1
1.2. TRIBOLOGY	8
1.3. WEAR.....	9
1.4. WEAR MECHANISMS.....	10
1.4.1. Abrasive Wear	10
1.4.2. Adhesive Wear.....	12
1.4.3. Fatigue Wear.....	13
1.4.4. Impact Wear.....	15
1.4.5. Corrosive Wear	17
1.4.6. Fretting Wear	18
1.5. PROBLEM STATEMENT.....	19
1.6. AIM AND OBJECTIVES	19
1.7. THESIS LAYOUT	20
CHAPTER TWO.....	21
LITERATURE REVIEW.....	21
2.1. WEAR PARAMETERS.....	21
2.1.1. Effect of Temperature.....	21
2.1.2. Effect of Load	26
2.1.3. Effect of Sliding Distance.....	28

2.2. CONCLUSION.....	29
CHAPTER THREE.....	30
EXPERIMENTAL WORK.....	30
3.1. MATERIAL SELECTION	30
3.2. TEST RIG.....	32
3.3. CALIBRATION THE EQUIPMENTS	37
3.4. SAMPLE PREPARATION	38
3.5. WEAR TEST PROCEDURE.....	40
3.6. TEST PARAMETERS.....	42
3.7. MECHANICAL TESTS	42
3.7.1. Hardness Test.....	42
3.7.2. Wear Test.....	43
3.7.3. Microstructure Observation.....	45
CHAPTER FOUR.....	46
RESULTS AND DISCUSSION	46
4.1. INTRODUCTION.....	46
4.2. FRICTIONAL HEAT	46
4.3 THE IMPORTANT CHARACTERISTICS OF WEAR BEHAVIOR AT DIFFERENT CONDITIONS	47
4.3.1. The Effect of Temperature on the Wear.....	47
4.3.2. The Effect of Applied Loads on the Wear.....	56
4.3.3. The Effect of Sliding Distance on the Wear.....	62
CHAPTER FIVE.....	67
CONCLUSIONS AND RECOMMENDATIONS	67
5.1. CONCLUSIONS	67
5.2. RECOMMENDATIONS FOR FUTURE WORK.....	68
REFERENCES.....	R1

LIST OF FIGURES

Figure 1.1 Abrasive wear, two body mode. Adopted from (Kovaříková <i>et al.</i> , 2009).....	11
Figure 1.2 Abrasive wear, three body mode. Adopted from (Kovaříková <i>et al.</i> , 2009).....	11
Figure 1.3 Steps leading to adhesive wear. (a) Microjoints. (b) Deformation of asperities and removal of surface films. (c) Shearing and material transfer. Adopted from (Podgornik, 2022).....	13
Figure 1.4 Pitting fracture caused by the load concentration, adopted from (Swain <i>et al.</i> , 2020).	14
Figure 1.5 Schematic of ductile material erosion technique (a): before impact, (b): crater development and piling material on one edge of the crater, (c): material separation from the surface, adopted from (Parsi <i>et al.</i> , 2014).15	
Figure 1.6 Erosion of compressor blades in gas turbine engine. From (Swain <i>et al.</i> , 2020).	16
Figure 1.7 Optical micrograph of a 52100 quenched and tempered roller bearing after corrosive wear (Tallian <i>et al.</i> , 1974).....	17
Figure 1.8 Signs of fretting wear on the surface of the wheelset axle from (Dębiński and Brezáni, 2018)	18

Figure 3.1 Figure of test rig machine.....	33
Figure 3.2 AC drive.....	34
Figure 3.3 Hot air gun	35
Figure 3.4 Temperature data logger	36
Figure 3.5 Tachometer	37
Figure 3.6 Dial gauge.....	38
Figure 3.7 A schematic of the pin specimen.....	39
Figure 3.8 Surface roughness measurement device	39
Figure 3.9 Surface of the pin specimen.....	40
Figure 3.10 Ball type micrometre	40
Figure 3.11 A digital vernier calliper.....	41
Figure 3.12 Electronic balance.....	41
Figure 3.13 Vickers hardness machine	43
Figure 4.1 Frictional heat during the wear test	47
Figure 4.2 Wear due to volume loss with temperature diagram for (Al2024, Al7075) at, a) 10 N, b) 20 N, c) 30 N.	49
Figure 4.3 SEM micrograph at constant applied load of 20 N and temperature of 25 °C for, a) Al2024, b) Al7075.....	50
Figure 4.4 SEM micrograph at constant applied load of 20 N and temperature of 125 °C for, a) Al2024, b) Al7075.....	51

Figure 4.5 SEM micrograph at constant applied load of 20 N and temperature of 225 °C for, a) Al2024, b) Al7075 52

Figure 4.6 Optical micrographs of worn pin surfaces of Al2024 and Al7075 at different loads and temperatures 55

Figure 4.7 Wear due to volume loss with applied load diagram for (Al2024, Al7075) at temperature, a) 25 °C, b) 75 °C, c) 125 °C, d) 175 °C, e) 225 °C..... 57

Figure 4.8 Specific Wear rate with Load diagram for (Al2024, Al7075) at temperature, a) 25 °C, b) 75 °C, c) 125 °C, d) 175°C, e) 225 °C..... 58

Figure 4.9 SEM micrograph at a temperature of 125 °C and applied load of 10 N for, a) Al2024, b) Al7075..... 59

Figure 4.10 SEM micrograph at a temperature of 125 °C and applied load of 20 N for, a) Al2024, b) Al7075..... 60

Figure 4.11 SEM micrograph at a temperature of 125 °C and applied load of 30 N for, a) Al2024, b) Al7075..... 61

Figure 4.12 Wear due to volume loss with sliding distance diagram for (Al2024, Al7075) at temperature, a) 25 °C, b) 75 °C, c) 125 °C, d) 175 °C, e) 225 °C..... 63

Figure 4.13 SEM micrograph at sliding distances of 1570 m for, a) Al2024, b)
Al7075 64

Figure 4.14 SEM micrograph at sliding distances of 2356 m for, a) Al2024, b)
Al7075 65

Figure 4.15 SEM micrograph at sliding distances of 3141 m for, a) Al2024, b)
Al7075 66

LIST OF TABLES

Table 3.1 Physical properties of Al2024 and Al7075 and 2507 duplex stainless steel (Meric, 2000; Sudagar, Venkateswarlu and Lian, 2010).....	30
Table 3.2 Chemical composition of Al2024, Al7075 and 2507 duplex stainless steel (wt. %). (From chemical composition test).....	31
Table 3.3 Results of calibration of motor speed by Tachometer.	37
Table 3.4 Wear test parameters used in this study	42

LIST OF ABBREVIATIONS AND SYMBOLS

AA	Aluminium Alloy
AISI	American Iron and Steel Institute
Al	Aluminium
Al ₂ O ₃	Aluminium Oxide
ASTM	American Society for Testing and Materials
EDX	Energy Dispersive X-ray
RPM	Revolution per Minute
SEM	Scanning Electron Microscopy

SYMBOLS

F	Load (N)
S	Sliding distance (m)
W_r	Wear rate due to volume loss (mm^3)
W_s	Specific wear rate (mm^3/Nm)
ρ	Density (g/cm^3)
ΔW	Wear amount (mm^3)

CHAPTER ONE

INTRODUCTION

1.1. INTRODUCTION

Aluminum is used in the manufacture of many important materials. It may be used with its purity or as an alloy. Pure aluminum is a pure, soft metal with low mechanical properties. While aluminum alloys are materials that consist of aluminum and some other materials (such as Copper, Zinc, magnesium, silicon, manganese, tin, lithium and others) to obtain new properties that combine the characteristics of the materials used in the formation of the alloy (Davis, 1993). To choose the correct alloy for the specific application, considerations must be given to its coating, formability, weldability, and corrosion resistance. Flexibility considerations the incorrect use of aluminum may cause problems, especially when compared to iron or steel (Davis, 1993, 1999; Kaufman, 2000).

Several factors contribute to the importance of aluminium alloys in engineering applications, including their high strength to weight ratio, and excellent corrosion resistance (Miller *et al.*, 2000; Yang *et al.*, 2014; Zhang *et al.*, 2014). The majority of engineering sectors, such as car and aerospace applications, are using them at the moment (Li and Starink, 2001; Yan *et al.*, 2013; Sagar, Suresh and Sampathkumaran, 2021). Automotive and aerospace manufacturers are demanding to use the 7000-series aluminum. High strength-to-density ratios, fracture toughness, and stress corrosion crack resistance are just a few of the many reasons for this (Immarigeon *et al.*, 1995; Heinz *et al.*, 2000; Williams and Starke, 2003). These alloys are primarily strengthened by precipitation hardening. Strengthening these alloys by adding more Zn, Mg, and Cu, the primary components of precipitation strengthening, increases their tensile

strength, but also reduces their hot workability in the same time (Bergsma and Kassner, 1996; McQueen and Celliers, 1997; Zhang *et al.*, 2007).

According to the composition of aluminium alloys, there are some types of aluminium alloys with their applications:

- 1xxx: Used mostly in the chemical as well as electrical industries for the precise control of its unalloyed composition.
- 2xxx: Aluminum alloys that are mostly consist of copper but may include additional elements, such as magnesium. As a result of their great strength (yield strengths up to 455 MPa, or 66 ksi), 2xxx-series alloys are commonly utilized in aircraft.
- 3xxx: Manganese-based aluminium alloys are utilized as general-purpose alloys in construction applications and a variety of products.
- 4xxx: Silicon-based aluminium alloys use for welding rods as well as brazing sheet.
- 5xxx: Alloys containing magnesium as the primary alloying element, which are utilized in gangplanks, boat hulls, and other marine-related items.
- 6xxx: Alloys mostly composed of magnesium and silicon, which are often used in architectural extrusions as well as automotive components.
- 7xxx: Alloys containing zinc as a primary alloying element (though additional metal components may be specified), such as copper, zirconium, magnesium, and chromium, are often utilized in airplane structural components and other high-strength applications. With yield strengths of up to 500 MPa (73 ksi), the 7xxx series alloys are the strongest aluminium alloys.
- 8xxx: Characteristic alloys with different compositions. lithium, Tin, and/or iron may be present in the 8xxx series alloys.
- 9xxx: To be used in the future.

Wrought alloys that constitute heat-treatable (precipitation-hardenable) aluminum alloys include the 2xxx, 6xxx, 7xxx, and some of the 8xxx alloys. (Davis and Park, 2001).

AL2024 alloy belongs to series 2xxx series of aluminum alloys that is one of the strongest alloys have many properties that required in the world of engineering and industry such as heat treatable as they remain preserving their strength and hardness, good wear resistance (Kaufman, 2000; Sherif et al., 2011) can be weldable in special conditions, and are non-toxic (Reddappa et al., 2011). In addition, aluminium alloy 2024 is a combination of copper, magnesium, manganese, and other small alloying elements. It is made mainly by hot extrusion and rolling. The hardness value, strength value and elastic modulus of Al2024 are quite high. Aeroplane construction, rivets, orthopaedic soles, and pulling wheels are just a few of the many applications for this alloy in the engineering sector(Kaçar, Atik and Meriç, 2003).

The following is a summary of the temper of aluminum processing products as indicated by various processing methods:

H: Work-hardening temper. It is applied to products that gain strength by work hardening. After work hardening, the product may (or may not) go through further heat treatment to weaken it.

O: Annealed condition. It is suited to processed products with the lowest strength after full annealing.

T: Heat treatment temper. It applies to items that undergo work hardening or not to achieve stability after heat treatment. The character T must be followed by one or more Arabic letters (Generally, it is heat treatment strengthened material).

W: Solution heat treatment temper. It is a very unstable temper. It is only relevant to alloys that have naturally aged at room temperature after solution

heat treatment. These codes simply indicate that the product is experiencing its natural aging process.

F: Free-machining temper. It may be used on products that don't have any unique needs for work hardening or heat treatment conditions during the forming process. The mechanical characteristics of items at this temper are not mentioned (Kaufman, 2000; Benedyk, 2010).

The technique for designating tempers is based on the main treatment sequences that are used to create various tempers and their variations. Subdivisions of the Basic T Temper. The first number(s) following the letter T designation indicates the specific combination of basic operations:

T1, cooled after a high temperature shaping process and naturally aged to a significantly stable condition. This description refers to products that, after an elevated-temperature shaping procedure like casting or extrusion, are not cold worked and whose mechanical characteristics have been stabilized by aging at room temperature. It also applies to products that are flattened or straightened after cooling from the shaping process, for which the effects of the cold work imparted by flattening or straightening are not accounted for in specified property limits.

T2, cold worked, naturally aged, and cooled from an elevated-temperature shaping process to a substantially stable condition. This variant refers to items that have undergone cold working specifically to increase strength after cooling from a hot-working like rolling or extrusion and whose mechanical qualities have been maintained by aging at room temperature. It also applies to products in which the effects of cold work, imparted by flattening or straightening, are accounted for in specified property limits.

T3, solution heat treated, cold worked, and naturally aged to a significantly stable condition. T3 is suitable for items that have undergone solution heat

treatment and have been especially cold worked to increase strength, as well as products whose mechanical characteristics have been stabilized by aging at room temperature. It also applies to products in which the effects of cold work, imparted by flattening or straightening, are accounted for in specified property limits.

T4, solution heat treated, naturally aged, and in a substantially stable condition. This designates products that have undergone solution heat treatment but have not been cold worked, and whose mechanical features have been stabilized by aging at room temperature. The effects of the cold work given by flattening or straightening are not taken into consideration in the specified property limits if the products are flattened or straightened.

T5, cooled after a high-temperature shaping process and artificially aged. T5 refers to products that, after an elevated-temperature shaping procedure like casting or extrusion, are not cold-worked and whose mechanical characteristics have been improved by precipitation heat treatment. If the products are flattened or straightened after cooling from the shaping process, the effects of the cold work imparted by flattening or straightening are not accounted for in specified property limits.

T6, artificially aged and solution heat treated. Products in this category are those that have not undergone cold working after solution heat treatment and those whose mechanical characteristics, dimensional stability, or both, are significantly enhanced by precipitation heat treatment. If the products are flattened or straightened, the effects of the cold work imparted by flattening or straightening are not accounted for in specified property limits.

T7, solution overaged or stabilized and solution heat treated. T7 refers to wrought products that have undergone precipitation heat treatment beyond the limit of maximum strength to provide some specific property, such as increased resistance to stress-corrosion cracking or exfoliation corrosion. It is applicable

to cast items that have undergone solution heat treatment and artificial aging to give dimensional and strength stability.

T8 refers to a metal that has been artificially aged, cold-worked, and subjected to a solution heat treatment. The products that belong to this category have undergone solution heat treatment, followed by cold working to increase strength, and have benefited greatly from precipitation heat treatment in terms of either mechanical qualities or dimensional stability, or both. The effects of cold work, including any cold work imparted by flattening or straightening, are accounted for in specified property limits.

T9, artificially aged, cold worked, solution heat treated. Items in this category have had precipitation heat treated, and then cold worked to increase their strength.

T10 has been cold-worked and artificially aged after being shaped at high temperatures. Products marked with the T10 designation have undergone precipitation heat treatment to significantly enhance their mechanical qualities after being hot-worked (such as rolling or extruding) and then cold-worked (to increase strength). The effects of cold work, including any cold work imparted by flattening or straightening, are accounted for in specified property limits (Cayless, 2013; Kaufman and Rooy, 2004).

In many sectors aluminum alloys encounter working circumstances that include wear and friction. As a result, the study of aluminium alloy's tribological behavior is becoming more important. A committee of the organization for economic cooperation and development in 1967 discovered a modern scientific field that is concerned only with friction, wear, and lubrication in surfaces that are relatively in motion called Tribology (Ellis, 1965). The wear mechanisms of aluminium alloys were explored by many researchers. The mechanism of wear switched from mixing/oxidation to delamination and eventually to severe metal wear, when the sliding speed as

well as load increased according to their findings (Singh and Alpas, 1995; Wilson and Alpas, 1996; Zhang and Alpast, 1997; Mu *et al.*, 2005; Yang *et al.*, 2015).

Wear is caused by a variety of basic procedures including corrosive, fatigue, adhesion, and abrasion effects. These mechanisms act together to degrade the materials (Lee *et al.*, 2014). There are several sorts of wear that exist in practice, there has been great debate regarding how to classify these various types of wear. A basic categorization has been adopted in this case, this depends on the mechanisms that are at act to cause wear damage (Gee and Jones, 1998).

Contact-motion causes a high rate of wear even at light loads, limiting its industrial applicability (Totik *et al.*, 2004; Taskin, Caligulu and Gur, 2008; Vaira Vignesh, Padmanaban and Datta, 2018; Vaira Vignesh and Padmanaban, 2018). Friction is the resistive force that happens when two tangent surfaces move in obverse directions when there is a compressive force between them that works on joining them together (Ellis, 1965).

For the last several years, a significant amount of work has been put into understanding the behavior of surfaces that are in sliding contact with one another as well as the process that results in wear. The behavior of wear on alloys is determined by many factors, including the mechanical properties of the material such as hardness, toughness, and ductility, the microstructure of the material including its shape, size, and composition and the service conditions, which include the load, sliding speed, counter-face material, and temperature, which they are the most important factors to take into consideration. Wear is a key problem that occurs for these alloys in industrial applications, and according to estimates, the direct cost of this issue changes between 1% and 4 % of the gross national product (Das and Mohanty, 2011).

The friction tests of pin-on-disc, block-on-disc, and ball-on-disc are commonly applied in a real sliding system to investigate a mating system's

tribological behavior and to help in recognizing the causes of wear with friction (Wang *et al.*, 2010). The pin-on-disc test has been frequently utilized. A revolving disc is forced against a static pin. The force required to restrict the pin within a tangential direction is commonly used to assess friction. The majority of these tests are carried out at room temperature. However, test systems have often been adapted for usage at elevated temperatures or in different situations (Gee and Jones, 1998).

1.2. TRIBOLOGY

Tribology is described as the theory and technique of contacting surfaces during relative motion. This has to do with every feature of friction, lubricating, and wear (John Williams, 2005). The term "tribology" comes from the Greek word *tribos*, which means "rubbing or sliding." An operational analysis approach is used in a development of research called tribology to solve issues of enormous economic relevance such as the maintenance, and wear of technological equipment that ranges from home appliances to spacecraft (Stachowiak and Batchelor, 2013). Friction and lubrication are required for the normal functioning of our skeleton's joints, walking, and holding items. Although the skeleton's joints have the ability to heal themselves by regeneration, the negative impacts of wear may occasionally prohibit them from functioning correctly if the lubricating systems in the joints become ineffective. The mechanical design tries to reduce friction in equipment such as motors by incorporating proper lubrication into their construction. However, significant friction is required for the traction and break of rubber automobile tires against road surfaces in order for them to function properly (Gohar and Rahnejat, 2018).

1.3. WEAR

Wear is defined as the procedure by which material is removed from a surface as a result of contact with another surface. Almost all machines degrade in terms of durability and reliability as a result of wear, and the options for developing more advanced machines are limited due to wear issues. Therefore, wear control has developed into a critical need for advanced and dependable technology in the future (Kato and Adachi, 2000). Wear is now one of the most often common industrial issues in engineering, because wear lowers operational efficiency by raising component replacement, oil consumption, and power losses rates. Industrial equipment often encounters wear caused by abrasive as well as metal-to-metal sliding situations. Wear classification may be made based on several criteria, including the rate of wear, the type of relative motion and the mechanisms of wear. In elevated temperature tribological systems, adhesion and abrasion have been recognized as the most prominent wear processes (Eyre, 1981). Wear can be chemical, known as corrosion, or mechanical, which is known as erosion. Metal wear results from the plastic deformation of surface material, in addition to the removal of particles that create wear debris. Wear in mechanical parts, along with other cycles including creep and fatigue, leads surfaces to degrade, gradually causing material deterioration or lack of applicability (Swain *et al.*, 2020). In certain circumstances, the amount of wear is the consequence of multiple common elements, most notably the relation between the corrosion rate and load, speed, friction coefficient, adhesion, hardness as well as tensile strength (Praharaj, 2009).

1.4. WEAR MECHANISMS

Although there is no universally accepted understanding of wear processes, much progress has been achieved since the previous belief that there were two main kinds of wear: adhesive and abrasive. Almost every material breakdown mechanism is now generally accepted as contributing to wear behavior (Eyre, 1981). Understanding the wear processes is critical for controlling each wear process effectively. This control may be implemented at the design stage if the active wear mechanism can be identified in advance. This control may also be applied subsequently, in the case that a tribological system has to be redesigned as a result of a failure of wear-induced (Straffelini, 2015). There are several types of wear mechanisms, however, the most common wear mechanisms are described below.

1.4.1. Abrasive Wear

Abrasive wear is the result of hard particles penetrating a surface and displacing material by way of elongated chips or slivers. Otherwise, the smooth surface gets roughened by loosely attached metallic particles and/or reasonably regular grooves (Eyre, 1981). Abrasive wear occurs when rough and strong materials slide on a softer surface, removing the softer component and eventually damaging the surface by fracturing or plastic deformation. Most metallic and ceramic components with significant toughness and rough particles end up in the soft material's plastic stage. Even metal contacts bend plastically when subjected to greater loads (Jeyaprakash, 2020).

There are primarily two different circumstances that might lead to abrasive wear. The first scenario, known as "two-body abrasion," takes place when two surfaces come into contact with one another. This kind of abrasion often takes place during mechanical operations including grinding, machining, and cutting, as seen in Figure 1.1. In the second scenario, the rough surface acts as the third

body. This third body is frequently a tiny particle of abrasive that is trapped between the two main surfaces, it is significantly harder to abrade one or both of the contact surfaces (three-body abrasion), as depicted in Figure 1.2. In several instances, the primary mechanism of wear is adhesive, and results in the formation of wear fragments that get stuck at the interface, causing abrasive wear of three-body. Scratching (often of the smooth surface) is seen in the majority of abrasive wear conditions as some grooves along the path of the slide (plowing). Scratching may be observed in the sliding direction. Scanning electron microscope (SEM) analysis of a cross-section of an abrasive wear sample revealed some underneath plastic deformation, although not as much as during adhesive wear. Furthermore, a 10–80% improvement in microhardness was found on worn surfaces (Bhushan, 2013).

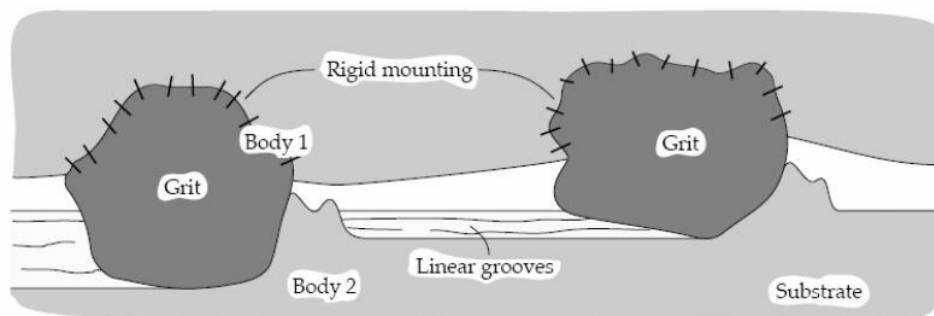


Figure 1.1 Abrasive wear, two body mode. Adopted from (Kovaříková *et al.*, 2009).

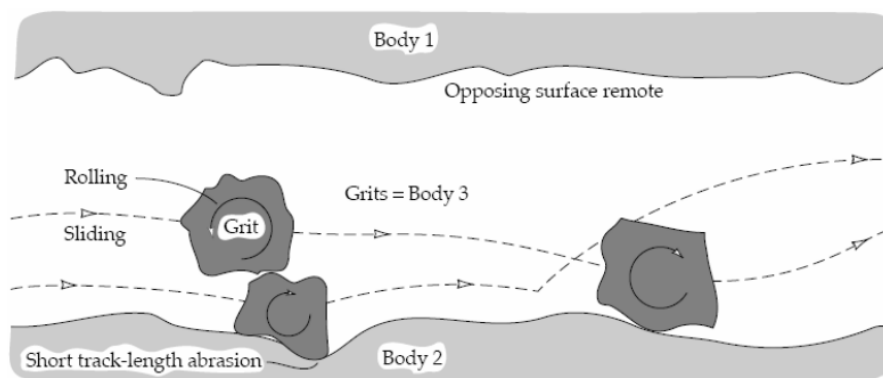


Figure 1.2 Abrasive wear, three body mode. Adopted from (Kovaříková *et al.*, 2009).

1.4.2. Adhesive Wear

Adhesive wear is the term given to the phenomenon that occurs when the forces of adhesion that exist among contacting asperities play a substantial role in the generation of wear fragments (Straffelini, 2015). Adhesive failure due to wear the scoring, galling, and scuffing modes are available. They form when microscopic protrusion at the sliding contact of two mating components weld together under conditions of high localized pressures and temperatures. After the metal has been welded together, sliding forces pull it away from one surface. As a consequence, a small cavity forms on one surface and the projection forms on the other, causing further damage. Thus, adhesive wear begins on a microscopic scale but advances on a macro scale. The simplest method for avoiding adhesive wear is to keep sliding surfaces away from metal-to-metal contact. It would be achieved via the application of a lubricant layer or other appropriate coatings (Geitner and Bloch, 2012). Wear rises when the asperity appears chemically pure, as welding and bonding are more probable, and wear enhances when the worn pair is mutually soluble. In addition, transfer and adhesion of metal might happen as a result of a harder surface asperity (steel) plowing through a soft counterface (bronze). With alloys, such as grey iron, adhesion is rare, and other mechanisms play a major role (Eyre, 1981). Shearing between two solid objects and the weaker surface of these surfaces is still a well-recognized mechanism for adhesion (Archard, 1953). Figure 1.3 shows the three steps that lead to adhesive wear. According to reports, the adhesive in reciprocating sliding situations causes a higher rate of wear than unidirectional sliding in similar situations. This is explained by cyclic forces acting on the material at the contacting object's surfaces (Dwivedi, 2010).

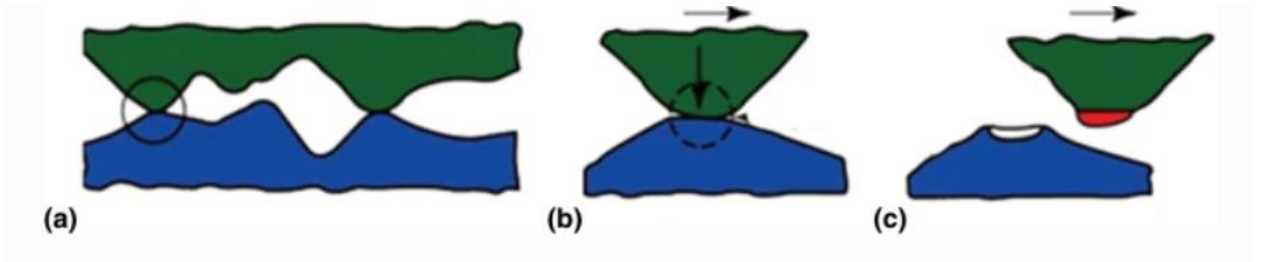


Figure 1.3 The progression of adhesive wear: (a) Microjoints. (b) Removal of surface films and deformation of asperities. (c) Material transfer and shearing. Adopted from (Podgornik, 2022)

Galling wear, scuffing wear and scoring wear are some types of the adhesive wear. Galling wear is a kind of surface degradation caused by sliding materials that are characterized by macroscopic, typically roughening, localized, and the formation of protrusions over the surface, This usually involves transfer of material, plastic flow, or a combination of the two (Gurumoorthy *et al.*, 2007). Scuffing wear is identified with a fast increase in surface temperature and also friction caused by the loss of the lubricant layer (Dyson, 1975; Ludema, C., 1984; Bowman and Stachowiak, 1996). It should be mentioned that adhesive wear is characterized by solid-state welding as well as material transfer (Izumi *et al.*, 2018). Additionally scoring wear is another severe type of adhesive wear, that arises as a consequence of tiny particles welding together as a result of the tooth mesh zone warming (owing to excessive contact pressure and/or sliding velocity), allowing surface-to-surface contact (Eyre, 1981).

1.4.3. Fatigue Wear

During repetitive rolling and sliding, subsurface, as well as surface fatigue, is detected. The repetitive cycles of loading/unloading might cause the development of surface or subsurface fractures, which ultimately result in the disintegration of the surfaces with the development of large pieces, leaving enormous pits within the surface. In the fatigue wear there is minimal wear, compared with the wear produced by abrasive and adhesive mechanisms, which results in progressive degradation from the beginning of the operation.

As a result, the quantity of material lost due to fatigue wear is a useless parameter (Bhushan, 2020). When surfaces are subjected to varying loads, they might wear due to fatigue. Great surface loads lead cracks to propagate deeper into the materials, and then if two or several of such cracks connect with each other, massive particle loss develops.

In general, fatigue wear on the surface or subsurface layer can be observed in a continual sliding as well as rolling atmosphere. The constant unloading and loading operations cause fractures to grow on the surface as well as subsurface after significant repetitive cycles. The surface of the material will eventually fracture into bigger pieces, which will result in the formation of greater pits on the softer material's surface (Jeyaprakash, 2020). The metallurgy of material is critical in avoiding bearing fatigue, especially at and near the surface. To improve fatigue resistance, a variety of surface treatments are used, including those that increase surface hardness while also creating residual compressive stress (Eyre, 1981). Figure 1.4 depicts the pitting fracture caused by the load concentration.

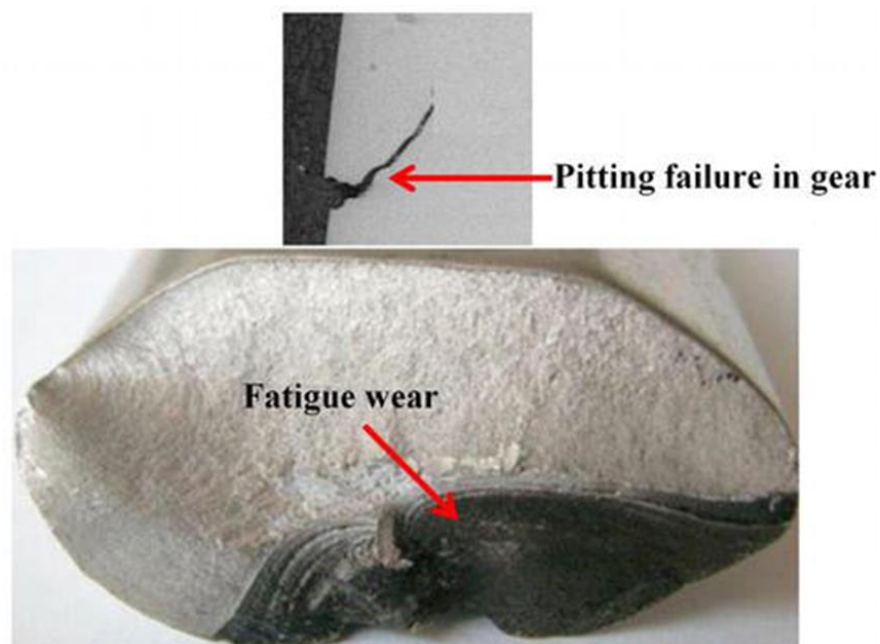


Figure 1.4 Pitting fracture caused by the load concentration, adopted from (Swain *et al.*, 2020).

1.4.4. Impact Wear

The impact is usually related to sliding for most practical equipment applications. The term "compound impact" refers to the surfaces' relative approach that are in contact, which includes both normal and tangential components. This category includes two distinct kinds of wear phenomena: percussive wear and erosive wear. Percussion is produced by repeated solid body collisions. Repeated collisions result in a gradual material loss (Engel, 1976). Erosion happens due to solid particles impinging on the surface. It may occur as a result of jets and the streaming of hard particulates, liquid droplets, or the implosion of fluid bubbles (Bhushan, 2013). The impinging particle's kinetic energy in erosive wear is determined by the abrasive sizes, particle velocity, and impingement angle. In erosion, as a result of repeated collisions, debris and wear particles are created (Finne, 1960). Erosion solid particle, fluid erosion and cavitation erosion are some kinds of impact wear. An example of impact mechanism wear depicted in Figure 1.5.

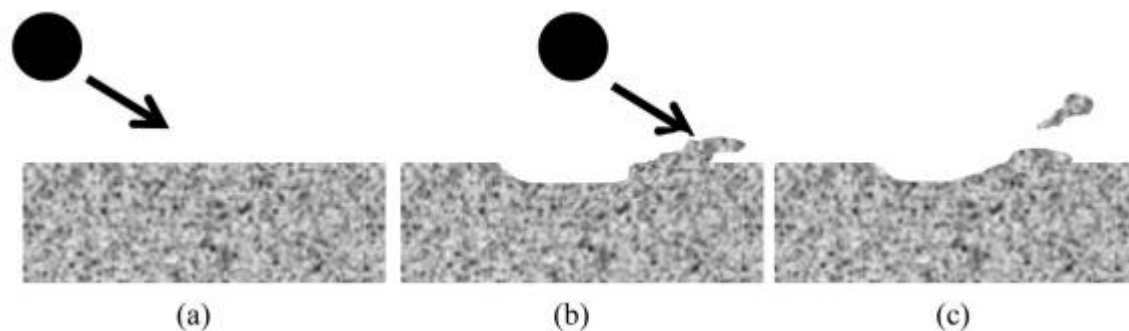


Figure 1.5 Schematic of ductile material erosion technique (a): prior to impact, (b): crater development and piling material on one edge of the crater, (c): separation of material from the surface, adopted from (Parsi *et al.*, 2014).

Since the word erosion is frequently utilized in association with conditions which may be best described as abrasion, the difference between the two should be made clear. Abrasion is the consequence of abrasive particles sliding over a surface in response to an externally applied force, whereas solid

particle erosion is the result of a down fall of particles impacting off the surface. The most noticeable difference is that in abrasion the force imposed on the material comes from outside sources and is relatively constant, but the amount of force applied to a material during erosion is proportional to the rate at which its particles lose speed (Kosel, 1992). An example of erosion by solid particle are shown in Figure 1.6.

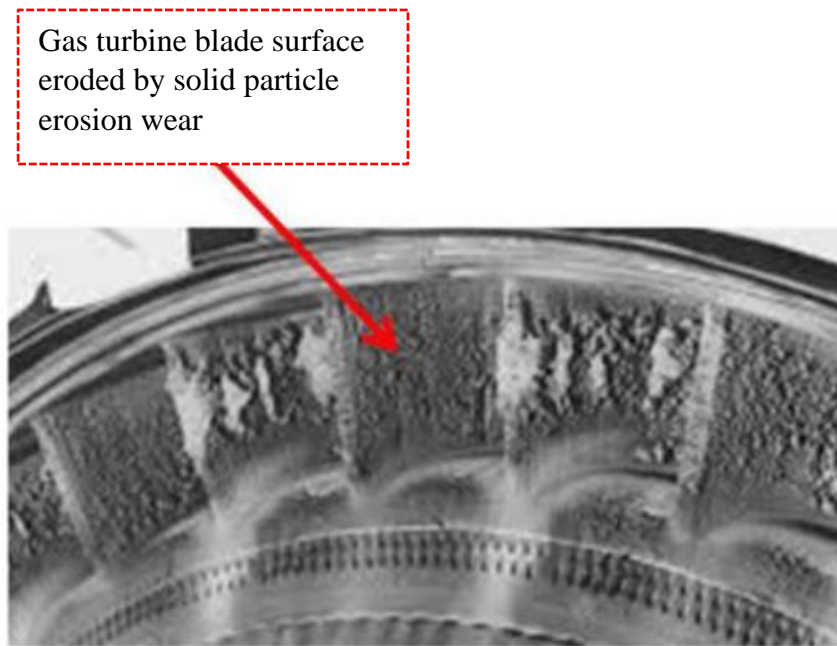


Figure 1.6 Gas turbine engine`s compressor blades erosion, adopted from (Swain *et al.*, 2020).

Cavitation erosion occurs when bubbles created in the fluid become unsteady and collide with the surface of the solid when a solid and fluid are moving relative to one another. This process causes damage to components such as ship propellers as well as pumps of centrifugal. The stability of bubbles is determined by the pressure differential between the bubble`s outside and interior, as well as the bubble's surface energy. Surface fatigue wear and cavitation erosion are quite similar, therefore materials that are resistant to one also are resistant to the other. This is especially true of materials that are hard but not brittle. However, cavitation resistance requires resistance to the liquid's corrosive attack (Bhushan, 2020).

1.4.5. Corrosive Wear

Corrosive wear also known as oxidation or chemical wear. Tribochemical interactions are between the surrounding media and the components of the contact surface, including a lubricant of liquid or air, are expected to produce thin coatings in the case of corrosive wear (Kato, 2014). In a chemical environment, corrosive or chemical wear which shown in Figure 1.7 occurs if sliding happens. In the air atmosphere, oxygen is supposed to be the most dominating corrosive medium. As a result, in an air atmosphere corrosive wear is commonly referred to as wear of oxidative. Wear of corrosive is crucial in several industries, including chemical processing, slurry handling, extraction, and processing of mineral. Chemical wear might occur as a result of electrochemical or chemical interactions between surfaces and the environment. However, chemical corrosive wear happens in highly corrosive environments, as well as in high levels of humidity and temperature environments (Wagner and Traud, 2006).

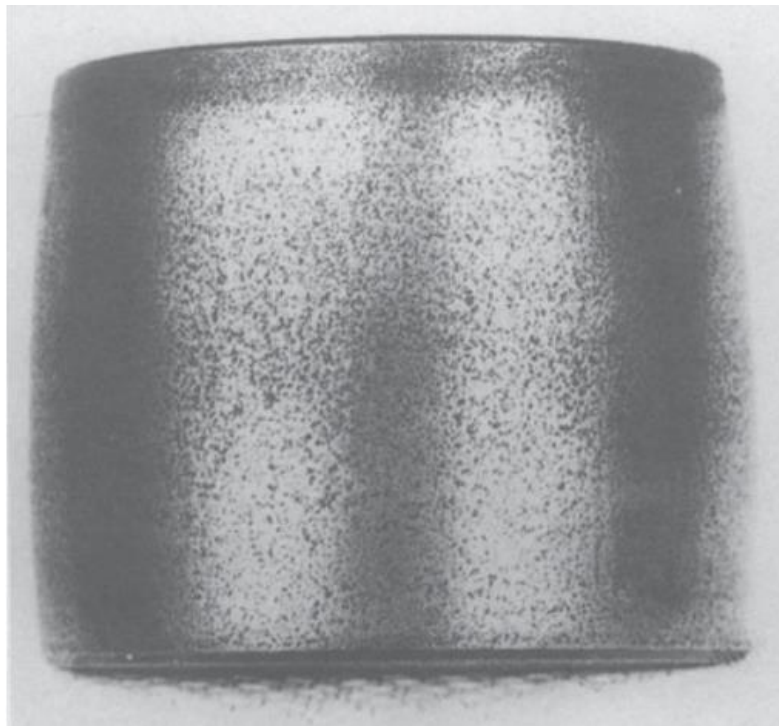


Figure 1.7 Optical micrograph of a 52100 quenched and tempered roller bearing after corrosive wear, adopted from (Tallian *et al.*, 1974).

1.4.6. Fretting Wear

Fretting happens when two metallic surfaces are loaded together and vibrate at low amplitudes (Waterhouse, 1981). It is a frequent occurrence, because the majority of equipment is exposed to vibration during both operation and transit. Shrink fittings, bolted parts, as well as splines, are all examples of vulnerable components. In fundamental, fretting is a kind of abrasive or adhesive wear in which vibrations cause wear debris as well as normal load produces adhesion among asperities. Fretting is often used in combination with corrosion, where regarding the wear phase is referred to as fretting corrosion. fretting wear may be greater than abrasive and also adhesive wear per unit of sliding distance. Fretted surfaces have a distinctive look with red-brown spots on ferrous materials and highly polished adjacent regions because of the lapping nature of rigid iron-oxide debris (Bhushan, 2013). Fretting wear, as seen in Figure 1.8, is a kind of surface damage that occurs on the axle of a wheelset.

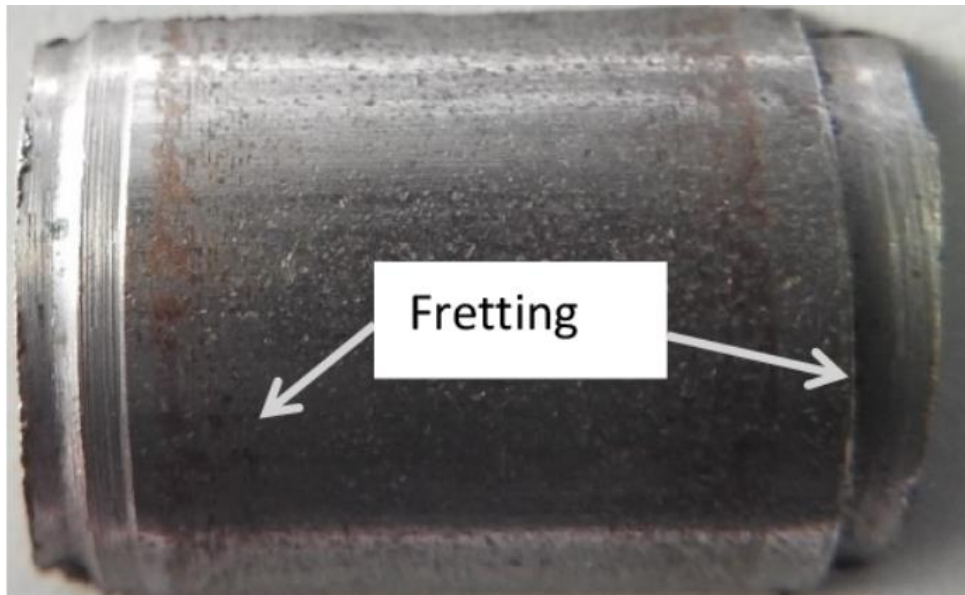


Figure 1.8 Signs of fretting wear on the surface of the wheelset axle from (Dębiński and Brezáni, 2018)

1.5. PROBLEM STATEMENT

The mechanical components, which are in contacts, in industry are subjected to high temperatures due to the friction. As a result, the wear behavior at high temperatures becomes critical (Mousavi, Abarghouie and Seyed Reihani, 2010). While the dry sliding wear behaviors of Al alloys are well documented at ambient temperatures, their wear characteristics at higher temperatures are different. The wear at high temperatures is a fundamental issue in a wide variety of industrial applications, including engine blocks, cylinder heads, and pistons, while some of these parts are frequently needed for running at temperatures approximately 200 °C (Muratoğlu and Aksoy, 2006). Also, there are several engineering applications where high-temperature tribology (the study of wear, friction, as well as lubrication) is critical, such as hot sheet metal forming, power generation, and aircraft (Singh, Kaur and Upadhyaya, 2019). At high temperatures, the wear behavior of metals as well as alloys is influenced by the conditions of use (Pauschitz, Roy and Franek, 2008; Rajaram *et al.*, 2010). Aluminium alloys are subjected to high temperatures in service. When paired to harder surfaces and exposed to high loads at higher temperatures, these alloys become sensitive to wear (Nie *et al.*, 1999; Arslan *et al.*, 2009).

1.6. AIM AND OBJECTIVES

The main aim of this study is to investigate the effect of temperature, load and sliding distance on the wear characteristics of two different types of aluminium such as Al2024 and Al7075 and comparison of the wear characteristics of these two alloys at different condition. For this purpose, a high-temperature pin-on-disc tribometer machine was designed and used at different conditions, including temperature, load and sliding distance, while the sliding speed was kept constant.

1.7. THESIS LAYOUT

This thesis is divided into the following chapter headings: Literature Review, Experimental Work, Results and Discussion, and lastly, Conclusions and Recommendations. A brief summary of each chapter is as follows;

- Chapter One: Introduction. It includes an introduction about aluminium alloys, wear, and wear mechanisms, the statement of the problem, and the aim of the current study.
- Chapter Two: Literature Review. It includes a review of the study of relevant literatures about wear of aluminium alloys at different conditions.
- Chapter Three: Experimental Work. It mentioned the test rig set-up, sample preparation, calibration of equipment, mechanical tests, microstructure observation, and experimental procedure.
- Chapter Four: Results and Discussion. The practical experimental results and the effect of elevated temperature on both aluminium alloys (Al2024, Al7075) are mentioned in this chapter with plotting.
- Chapter Five: Conclusions and Recommendations. It includes the conclusion and findings from the experimental work, and also includes the recommendation for future work.

CHAPTER TWO

LITERATURE REVIEW

2.1. WEAR PARAMETERS

2.1.1. Effect of Temperature

Wear at high temperatures is a major issue in many different types of industrial applications. Some experiments were done to assess the impact of different temperature on the Al alloys wear characteristics:

In the experiment conducted by Singh and Alpas in 1995, experiments of dry sliding wear were conducted on the Al 6061 alloy at higher temperatures. When the temperature of the surrounding environment is raised over a specific limit, the Al 6061 alloy, displayed a moderate to severe wear transition. During very high temperatures, plastic deformation, as well as material transfer, lead to a significant increase in wear.

On the other hand, Martin, Martinez and Llorca in 1996 , assessed how the wear resistance of a 2618 Al alloy is influenced at the temperatures ranging from 20 to 200 °C. According to the findings, with enhancing temperature the rate of wear of the alloy increased. A mild to severe wear transition was seen and the transition temperature of the alloy was between 100 and 150 °C.

Martin, Llorca and Rodriguez in 1999, considered the impact of temperature on the wear properties of 6061 and 2014 Al alloys. Using a tempered steel as counterbodies, wear experiments were conducted in a machine of oscillating friction throughout the temperatures between 20 and 200 °C for investigating the impact of temperature on the wear behavior of both aluminium alloys. Tests were performed to measure the wear resistance as well as friction coefficient with temperature. From the results it seems that plastic deformation of the alloy has the responsibility of the wear process, and at the temperatures 25 °C to 125 °C the rate of wear is constant, but after that with

enhancing temperature the wear rate increases. As can be seen, with enhancing temperature both materials exhibit a significant rise in friction coefficient.

A study by Muratoglu and Aksoy in 2000 was carried out in a block-on-disc device at various temperatures to evaluate the behavior of friction and wear for 2124 aluminium alloy over AISI 1050. At a velocity of 2 *m/s*, the sliding wear examinations were conducted. Dry sliding experiments and lubricated slide tests were conducted, under the load of 52 and 312 *N*, respectively. A number of samples were heated to temperatures between 25 and 200 °C, and wear experiments were conducted on them for evaluating the impact of temperature on the wear behavior of the alloy under consideration. In dry sliding testing, it was discovered that the temperature of 100 °C served as a transition point for both wear rate and wear processes. The transition temperature for alloy was determined to be 100°C when all other test temperatures were considered. The rate of wear increases as the temperature increases.

Also, the experimental test was done by Natarajan *et al.* in 2009 , to investigate the wear rates of Al 6063 at both ambient and elevated temperatures. A dry slide wear behavior of alloy has been studied at different temperatures (300, 200, and 100 °C) utilizing the pin on disc technique under varied used loads of 29.4, 19.6, and 9.8 *N*. In addition, comparative research at ambient temperature was conducted. The findings show that the Al 6063 alloy's wear resistance decrease with increasing temperature.

A study by Abarghouie and Reihani was conducted in 2010 for investigating variations in wear resistance of the alloy Al2024 throughout a range of temperatures 25–250 °C. In artificially aged Al2024, the wear and friction properties were studied throughout temperatures ranging from 20 to 250 °C. A pin-on-disc device is applied for evaluating dry sliding wear under conditions of a 20 *N* applied force and constant sliding velocity (0.5 *m/s*).

Surfaces that were worn and debris from wear were also observed utilizing SEM and EDX. According to the findings, the aged 2024 aluminium alloy exhibited the lowest wear values around 25 °C and subsequently experienced an increase in wear with rising temperature. All specimens exhibited a wear transition that ranged between mild and severe, the 2024 Al alloy had severe wear when exposed to 125 °C.

On the other hand, Qutub *et al.* in 2010, at high temperatures (25 °C–300 °C) determined the tribological behavior of 6061 aluminium. The effect of temperatures on wear properties of 6061 Al alloy on an AISI 4041 steel disc was investigated. The load of 15 N, 30 N, and 40 N were used, at a temperature of 300 °C, 200 °C, and 100 °C. According to the findings, with increasing temperature owing to alloy softening, the wear resistance of alloy reduces.

A study by Kumar *et al.* in 2010 was conducted to determine the rate of wear at elevated temperatures in 6061 Al alloy during dry sliding. To examine the dry sliding wear characteristic of alloy under a load of 14.6 N at three different temperatures (300, 200, and 100 °C), the pin-on-disc technique was applied. In order to be a source of comparison, the investigation was also conducted at ambient temperature. The findings showed that with enhancing temperature the rate of wear increased and also the transition from moderate to high wear of 6061 Al alloy occurred within a temperatures range between 200 and 300 °C as a consequence of significant plastic deformation of the alloy.

Moreover, In 2010, Rajaram *et al.* carried out an experimental to investigate the characteristics of dry sliding wear for Al-Si alloys at ambient and elevated temperatures. The trend indicated that as the temperature increased, the rate of wear decreased. At the elevated temperatures, the decrease in rate of wear was attributable mostly to the development in oxide and glazing layers. During high-temperature sliding, oxidation-related wear was predominant.

In addition, Rajaram, Kumaran and Rao in 2010, investigated wear characteristics of Al-Si alloy at temperature ranges between room temperature to 350 °C. Stir casting was used to produce the Al-Si alloy. Wear testing revealed that the wear resistance of Al-Si alloy enhances with an increase in temperature. Oxidational wear happened mostly while sliding. According to the findings, with a rise of operating temperature, the alloy's wear resistance increases linearly. Such an impact, at elevated operating temperatures, is caused by the faster development of glazing layers and oxide films on sliding components.

In the experiment conducted by Rajan *et al.*, in 2014, the influence of the temperature on the wear rate and a worn surface for 7075 Al alloy was investigated. Applying a device of pin-on-disc, the alloy's sliding wear behavior was examined. The findings showed that once the ambient temperature was raised, the alloy's wear rate also increased. At elevated temperatures, alloy had a poorer resistance to wear. The applied temperatures have a considerable influence on the mechanism of wear. At elevated temperatures, the metal flow was detected, whereas, at ambient temperature, the wear mechanism has found to be abrasive.

On the other hand Yang *et al.* in 2015, examined the performance of 7075 aluminium alloy. The wear properties of dry sliding of the 7075 aluminium alloy were assessed in load conditions of 25–250 *N* and temperatures of 25–200 °C. Under different testing circumstances, the wear behaviors and processes were examined. A change in the load between the temperatures of 25 to 200 °C is accompanied by a change between mild and severe wear. Al7075 alloy is able to maintain a high level of wear resistance at high ambient temperatures and under low load. Adhesive and abrasive wear are the most common types of wear seen at room temperature. According to the findings, by increasing temperature the wear rate increases.

In addition Kumar, Kumaran and Kumaraswamidhas in 2016 investigated how the Al 2618 behaves under different temperature circumstances. Therefore, they examined the wear rates, the wear resistance, the friction coefficient, and the rates of specific wear under different circumstances. Applying the scanning electron microscope (SEM), the surface morphology was analyzed both before and also after wear testing. What was discovered based on the findings was that the highest wear resistance was obtained in ambient temperature throughout all output circumstances. Increasing temperatures causes the alloy's wear rate to increase, which suggests that additional wear processes are in operation. Transactions of moderate to severe wear are possible as a result of increasing temperature.

Dabral *et al. in 2017* examined the wear behavior of aluminium 6061 in dry sliding, at ambient temperature and higher temperature under various conditions. In their study, they discovered that as the temperature increased, the particular rate of wear in the alloy increased. The explanation for the higher rate of wear in high temperatures might be associated with the lack of wear resistance resulted from the alloy softening at these temperatures. When the temperature of the sample was increased, the specimen wear behavior alerted from abrasive to delaminating. At ambient temperature, abrasion-induced wear is more noticeable, but at high temperatures, delamination-induced wear is more noticeable.

On other hand, Bhaskar in 2018, at high temperatures (200, 250, and 300°C) explored the wear of Al 6061 alloy. The research is through a 50 m test path, with a reciprocating velocity ranging between 0.4, 0.6 m/s slid and the loads between 15 and 75 N utilizes in the investigation. At all different loads examined, a temperature rise caused the rise of in material loss.

2.1.2. Effect of Load

The normal load is one of the most effective parameters which greatly impacts the wear behavior of materials. Some tests were carried out to investigate the effects of load on the wear behavior of Al alloys:

Singh and Alpas in 1995, performed wear experiments to investigate the influence of load on the wear behavior of Al 6061. The experiments were conducted in dry conditions and at elevated temperatures. The alloy's wear rates in the moderate and severe wear regimes both increase when the applied load has increased from 10 to 50 *N*. Testing the alloy at 50 *N* reveals wear rates that are around 130% higher under the moderate wear regime. Wear rates at a specific temperature are proportional to the load being applied so, at any specific temperature, increasing the load will cause a rise in wear.

The experimental test was done by Natarajan *et al.* (2009), they conducted an experiment to evaluate the wear behavior of Al 6063 alloy. The pin-on-disc method was used to study the dry sliding wear behavior of the alloy at different temperatures and under different loads of 9.8, 19.6, and 29.4 *N*. The findings show that the rate of wear increases as the applied load is enhanced.

On the other hand, Qutub *et al.* (2010) examined the tribological characteristics of 6061 aluminium alloy at various temperatures. The study explored the influence that the load had on the wear characteristics of 6061 Al alloy against a steel disc of AISI 4041. As the load increases, so does the wear rate of the alloy. However, between 15 *N* and 20 *N*, a change zone from moderate to high wear is seen. The transition region begins at an applied force of 15 *N*.

In addition, Siddesh and Ravindranath in 2014, according to the ASTM G 99-95 standard, conducted a test of dry sliding wear on Al 2219. Pin-on-disc equipment was utilized for performing the wear experiments. At a constant sliding speed of 3.768 *m/s* and a sliding distance of 1500 *m*, the findings

demonstrate a considerable variation in wear rate according to the loading conditions. The wear rate dependably enhances since the pressure at the pin and disc contact rises in proportion to the applied load.

In addition, Yang *et al.* in 2015, examined the 7075 - Aluminium alloy performance. At the temperatures (25 to 200 °C) and under load circumstances ranging from 25 to 250 N, the dry sliding wear characteristics of the 7075 aluminium alloy were studied and evaluated. At any given temperature, a rise in the load would cause a rise in the amount of wear loss. It is obvious that the change from moderate to high wear takes place as the load increases. The wear is quite mild, if the load is low, but if it is high, it may become severe. When the load is increased further, the surface that has been worn becomes a polish surface. As the load is increased, the 7075 Al alloy exhibits a wear mechanism that may shift from moderate to severe. They discovered that when the load increased, the process of wear shifted from mixing and oxidation to delamination, and then eventually to severe metal wear.

Furthermore, in 2018 Bhaskar investigated the load impact on the dry wear characteristics of Al 6061 alloy. The reciprocating tribometer is used to measure the alloy wear behavior at the loads from 15 N to 75 N. Due to a rise among the material surfaces in the actual contact area, the study discovered that throughout the range of temperature and sliding velocity with a rise in applied load the wear rate of Al 6061 raised. High plastic deformation in the asperities causes the amount of wear debris creation, leading to a greater wear rate and the observed trend of wear loss when utilized load enhances.

2.1.3. Effect of Sliding Distance

Numerous studies have been conducted to investigate the impact that sliding distance has on the wear behavior of aluminium alloys:

Lee *et al.* evaluated the behavior of wear in aluminium alloy under various conditions using the dry sliding wear test in 1992. This test demonstrates the effect of sliding distances on weight losses in 6061 aluminium alloy. The weight losses in the alloy increase linearly as the sliding distance increases.

In 2000, a study was carried out by Muratoglu and Aksoy to examine the wear behavior of Al2024 over AISI 1050 steel using a block-on-disc tribometer device. The study was conducted at a velocity of 2 *m/s* and at two different loads (52 and 312 *N*). The sliding wear experiments were performed under dry and wet conditions. The results show that sample weight was reduced as the sliding distance increased.

Basavarajappa *et al.* (2006) examined the wear behavior of aluminium 2219 cast alloy, at variations of sliding distances in dry conditions. Based on the findings, it was revealed that aluminium alloy's wear rate rises with the sliding distance. In addition, Rao *et al.* (2009) carried out an experimental investigation on the aluminium alloy (Al–Zn–Mg) using a pin-on-disc tribometer at different pressures (0.2-2 MPa) and a constant sliding speed of 3.35 *m/s*. As a counter disc, they used EN32 steel. The results showed that the wear rate increased until the sliding distance of 1000 *m* and then remained constant until the sliding distance of 3000 *m*. It was seen that the alloy wear rate had a significant increase when increasing the sliding distance from 3000 to 4000 *m*. However, as the sliding distance increases, the subsurface deformation increases. Further increases in sliding distance result in higher temperatures, which in turn produce subsurface softening and plastic incompatibility.

Siddesh and Ravindranath (2014) examined a dry sliding wear test for Al 2219 according to the ASTM G 99-95 standard. The examination was performed using a pin-on-disc device with different parameters such as load, sliding velocity, and sliding distance. The findings demonstrate that the rate of wear rises when the sliding distance increases.

Previously, numerous researchers studied the wear characteristics of various types of aluminium alloys, as well as alloys reinforced with other particles, at room temperature and at elevated temperatures. The present research, explores the effects of elevated temperatures on two different types of aluminium alloys, namely, Al2024 and Al7075 for the first time. This work intends to add to this emerging field of research by investigating and comparing the wear behavior of these two different alloys

2.2. CONCLUSION

In this chapter, the previous research studies which examine the influence of various temperatures, loads, and sliding distances on the wear behavior of different types of aluminium alloy were described. From the result of these studies, the wear in aluminium alloy increases with rising temperature, load, and sliding distance. The next chapter describes the experimental work of this study.

CHAPTER THREE

EXPERIMENTAL WORK

3.1. MATERIAL SELECTION

As mentioned in chapter 1, because of their great strength-to-weight ratio, aluminium alloys are widely employed in a diverse use in industry, including components of automobile, the military sector, and aerospace. In the current work, the tests were conducted on different types of aluminium alloys including (Al2024 and Al7075). Duplex stainless steel (AISI 2507) was used to manufacture the counterpart disc. Table 3.1 presented the physical properties of the materials that selected for this study.

Table 3.1 Physical properties of Al2024-T6 and Al7075-T6 and 2507 duplex stainless steel (Meric, 2000; Sudagar, Venkateswarlu and Lian, 2010).

Materials	Ultimate Strength, MPa	Yield Strength, MPa	Shear Strength, MPa	Fatigue Strength, MPa	Modulus of Elasticity, GPa	Shear Modulus, GPa	Hardness, HV	Melting point, °C	Density, g/cm³
Al2024-T6	469	324	283	138	73.1	28	140	502 –638	2.78
Al7075-T6	572	503	331	159	71.7	26.9	189	477 - 635	2.81
AISI 2507	799	551	–	802	200	77	233	1205-1370	7.8

The chemical composition test was done for both aluminium alloys and also for the disc using (X-MET 7500) portable X-Ray device, to analyze the composition of them. The results of chemical composition of Al2024, Al7075 and 2507 duplex stainless steel are mentioned in Table 3.2.

Table 3.2 Chemical composition of Al2024, Al7075 and 2507 duplex stainless steel (wt. %). (From chemical composition test of specimens)

	Cu %	Zn %	Mg%	Fe%	Si%	Mn%	Cr%	Zr%	Ti %	Ni%	Mo%	Co%	P%	S%	C%
Al2024	4.84	–	0.55	0.25	0.33	0.65	0.05	< 0.00		–	–	–	–	–	–
Al7075	1.55	5.88	1.45	0.63	<0.00	–	> 0.28	–	0.08	–	–	–	–	–	–
AISI 2507	0.065	–	–	–	0.363	1.6	23.46	–	–	5.16	2.93	0.133	0.0171	0.0049	0.065

3.2. TEST RIG

A high-temperature apparatus of pin-on-disc tribometer was designed and manufactured for studying the wear behavior of the Al2024 and Al7075 at elevated temperatures. The test setup for this investigation is shown in both schematic and photographic form in Figure 3.1. The tribometer machine consists of a solid flange made from low carbon steel with 20 *mm* thickness and 150 *mm* diameter. The counterpart disc made from 2507 duplex stainless steel attached to the flange using three bolts. Also, a long vertical shaft was gripped with a bolt from the bottom of the flange. The shaft rotates through a bush-bearing that is tightly connected to a solid flange and 2507 duplex stainless steel disc. A V-pulley below the flange was fixed with the shaft and connected to the motor by a belt for transmitting rotation from a motor to a shaft. The motor has a power of 0.75 *hp* and a maximum speed of 1365 *RPM*. There is a holder in which a cylindrical pin can be mounted on it. It is possible to change the sliding speed in two different ways: either by adjusting the frictional radius or changing the speed at which the shaft is rotating. In this experimental study, the sliding speed is controlled through altering the motor's rotating speed, where keeping a frictional radius of exactly 50 *mm*.

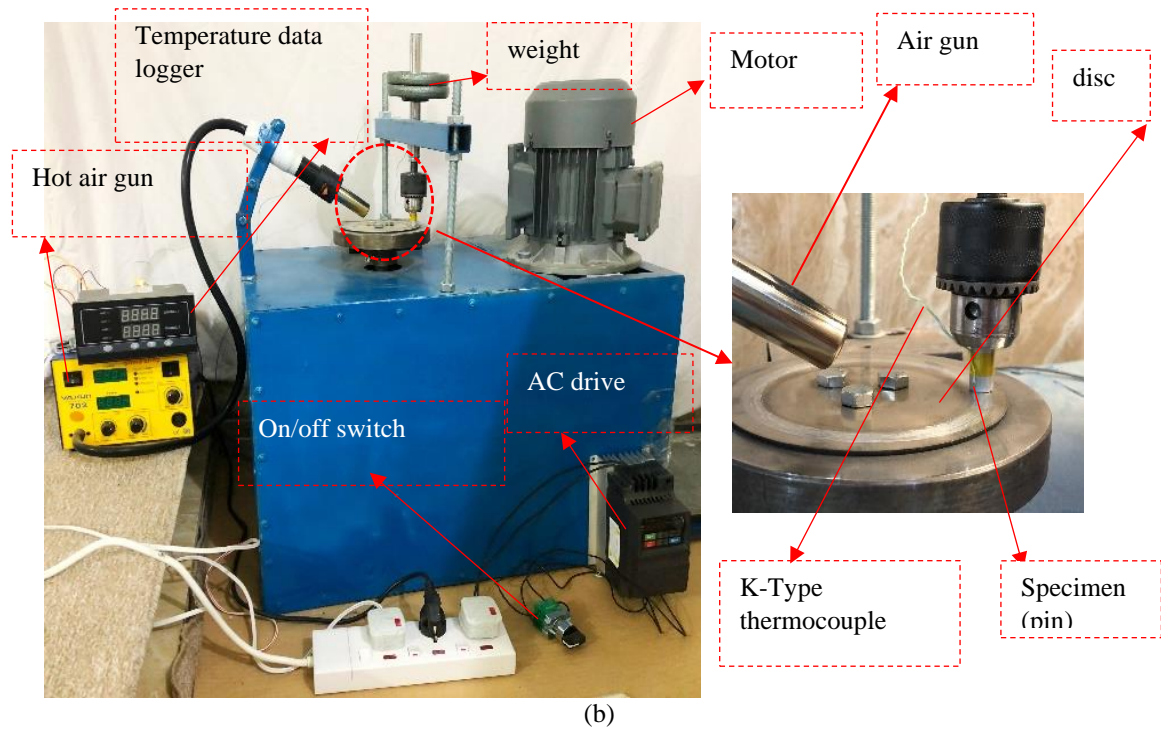
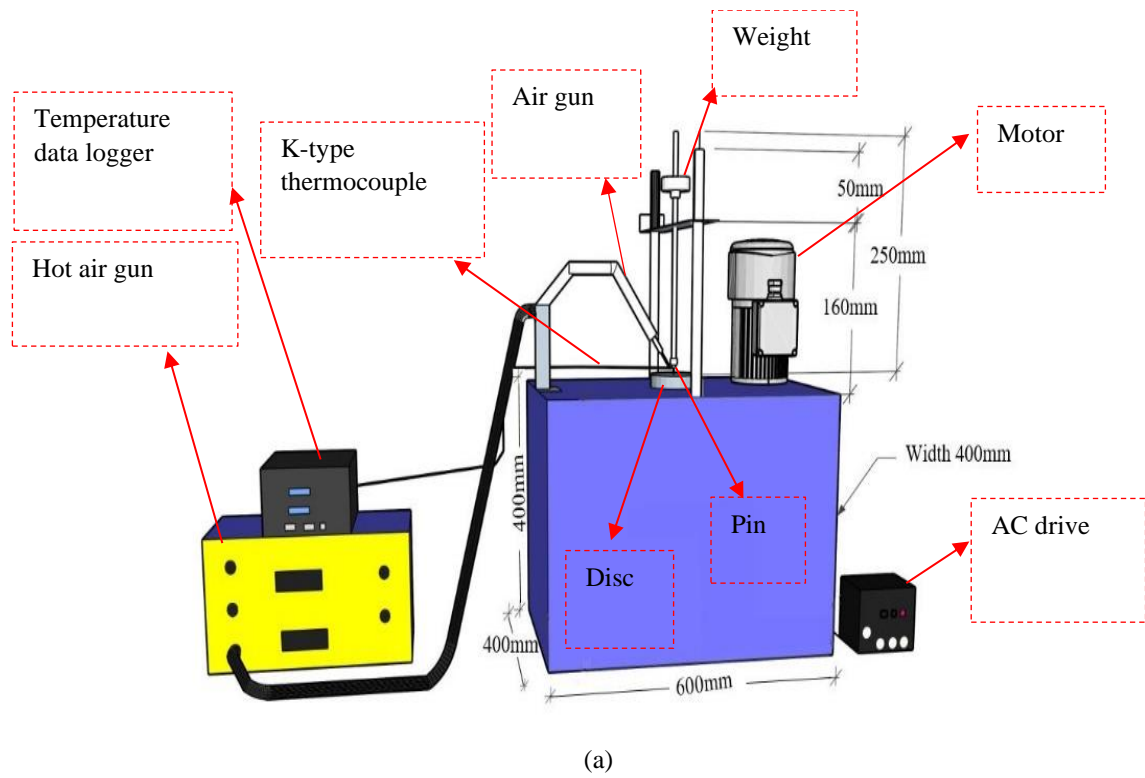


Figure 3.1 Figure of test rig machine

Motor speed can be varied according to the condition by the use of AC drive Type (Delta VFD EL-W) which is a device that controls the frequency of the motor. Figure 3.2 shows the AC drive used in this study, which consists of the plug to turn on/off the device. There is also a controller to increase or decrease the *RPM* of the motor.

The RPM of the machine can be found by this equation

$$\frac{\text{Maximum RPM of motor}}{\text{Frequency}} = \text{Constant number} \quad (3.1)$$

$$\text{RPM during the test} = \text{Frequency} \times \text{constant number} \quad (3.2)$$

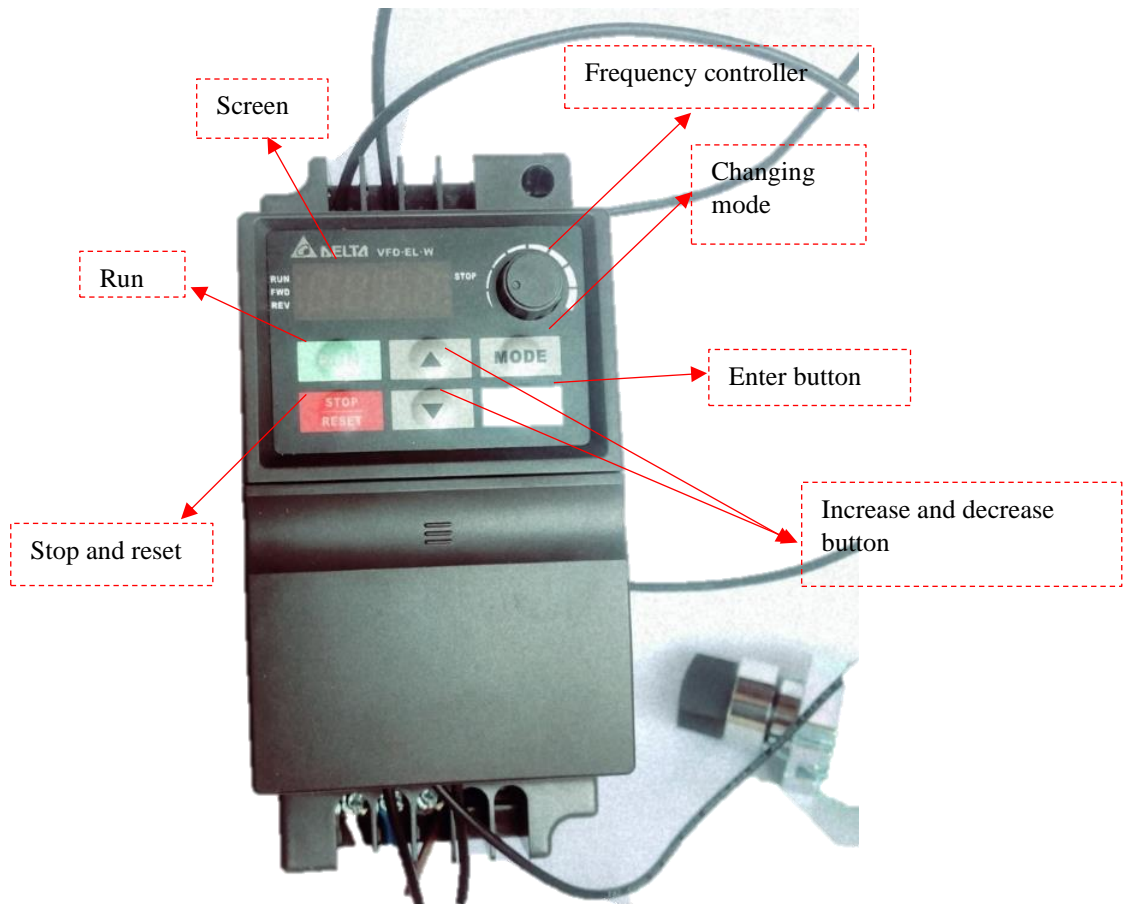


Figure 3.2 AC drive

To examine the effect of temperature, a hot air gun, as shown in Figure 3.3 was used. The gun produces a flow of hot air with a temperature higher than 400 °C. The shape of a heat gun is that of an extended body that is used to direct heat toward a target. A heat gun is made up of several parts: a source of heat, which is an electrical heating element; a mechanism for moving the hot air, which is usually an electric fan. A nozzle for directing the air, which could be a simple tube trying to point in a certain direction and particularly shaped for a specific purpose. It can concentrate the hot air on a small space; and a mechanism for turning it on and off, which is a trigger.



Figure 3.3 Hot air gun

A thermocouple (K-type) that was attached to the specimen side near the contact surface to measure the temperature during the wear test. (See Figure 3.1).

By applying (KCM-TF) data logger with two channels, the temperature data was gathered using SD card. The temperature data recorded with a sample period of *1 sec*. The data logger is shown in Figure 3.4.

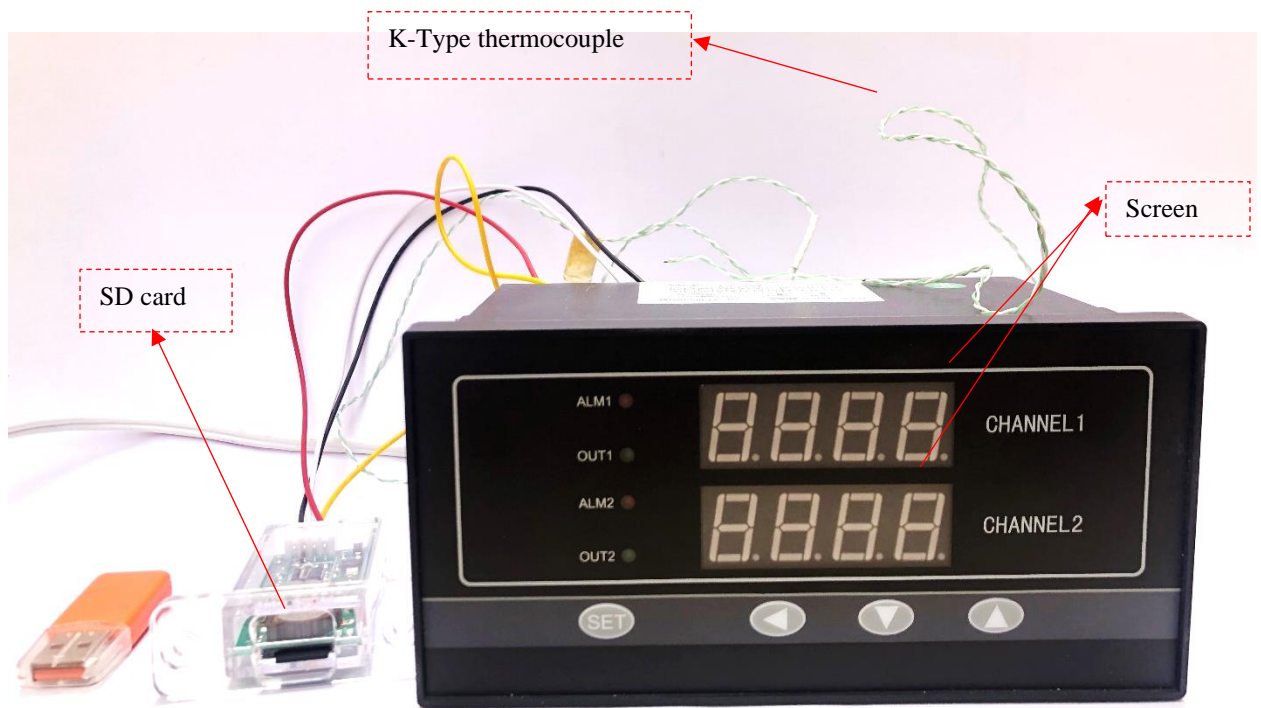


Figure 3.4 Temperature data logger

3.3. CALIBRATION THE EQUIPMENTS

For calibration and to checking the accuracy of the AC drive, a tachometer (shown in Figure 3.5) has been used to compare the *RPM* of AC drive and the *RPM* recorded by the tachometer. The revolutions per minute (*RPM*) of the device can be measured by directing the tachometer to the rotating shaft or disc. At first to check the accuracy of the tachometer, the lathe machine turned on at a specific speed and the tachometer is used to read the speed of the rotation. Table 3.3 has illustrated the results of the calibration.



Figure 3.5 Tachometer

Table 3.3 Results of calibration of motor speed by Tachometer with %6 of error ratio.

Frequency (Hz)	SET RPM (by equation)	ACTUAL RPM (Tachometer)
18.3	500	530
27.4	750	798
36.6	1000	1070
45.78	1250	1338
50	1365	1466

The flange which rotates beneath the pin specimen during the test was calibrated using a dial gauge, to measure the flatness of the flange (shown in Figure 3.6).

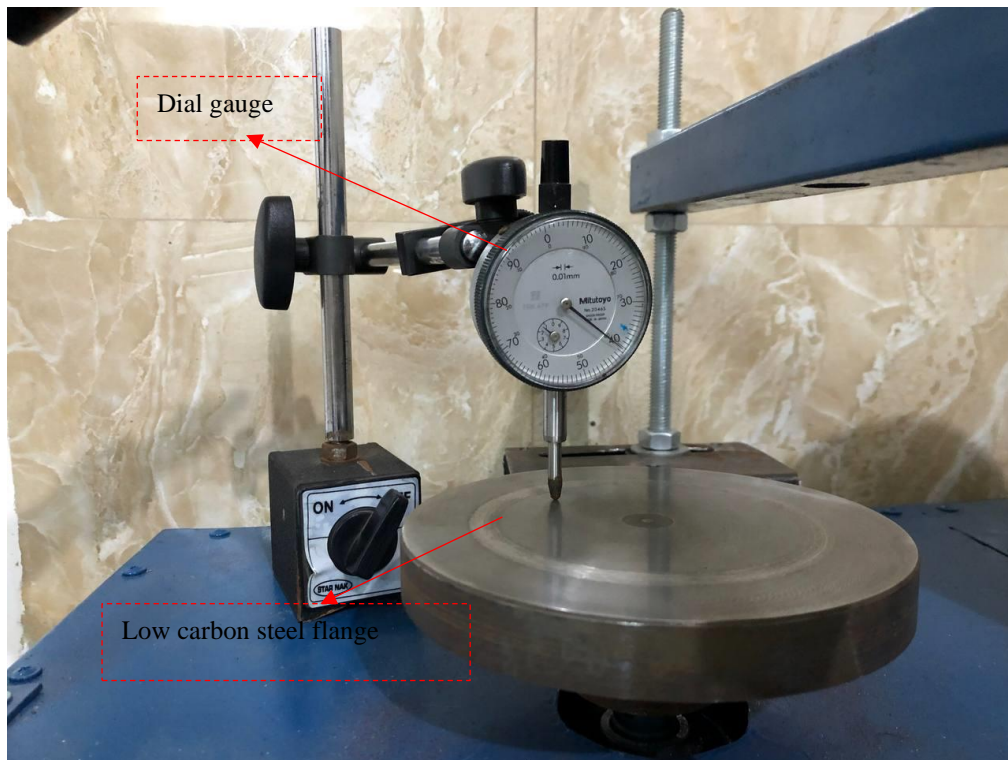


Figure 3.6 Dial gauge

3.4. SAMPLE PREPARATION

The Al2024 and Al7575 rod was machined, using a lathe machine, to prepare the pin specimens based on the standard of ASTM G99-17, with a 30 mm length and 10 mm diameter. The pin specimen is shown schematically in Figure 3.7. In addition, with a 3 mm thickness and a 120 mm outside diameter, the disc of counterpart was manufactured. To eliminate scratches and machining marks, the specimens were mechanically ground using 800, 1500, 2000, and 3000 grit abrasive sheets and trading silicon polish paste used for polishing to surface roughness of 0.03 μm which has been measured using Tyler-Hobson surface roughness tester (Talysur-10) shown in Figure 3.8. And the surface of the pin specimen shown in Figure 3.9. Before and after every

test, the pin specimens are cleaned with the use of acetone and dried with hot air.

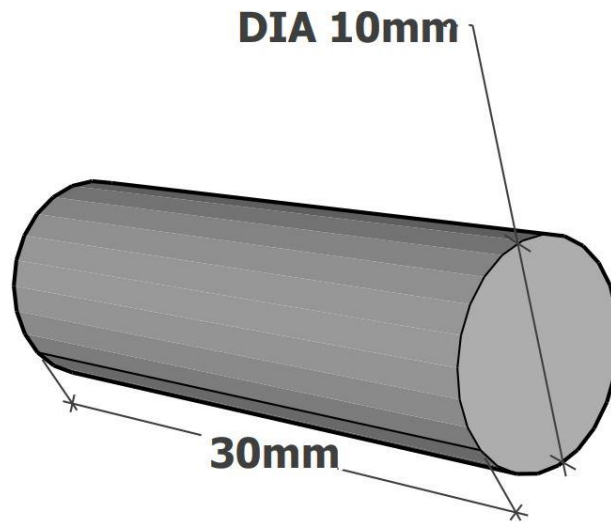


Figure 3.7 A schematic of the pin specimen



Figure 3.8 Surface roughness measurement device (Talysur-10)



Figure 3.9 Surface of the pin specimen

3.5. WEAR TEST PROCEDURE

The diameter of the pin specimens of (Al2024, Al7075) was measured using a ball micrometer (shown in Figure 3.10), while for measuring the pin length before and after each test a digital Vernier calliper was used. Figure 3.11 shows a digital Vernier caliper.



Figure 3.10 Ball type micrometre



Figure 3.11 A digital vernier calliper

Before and after each test the weight of the pin was measured utilizing a digital scale (model KERN ABJ-NM/ABS-N) with resolution of 0.0001 g. Figure 3.12 illustrates the scale that was utilized in the current work.

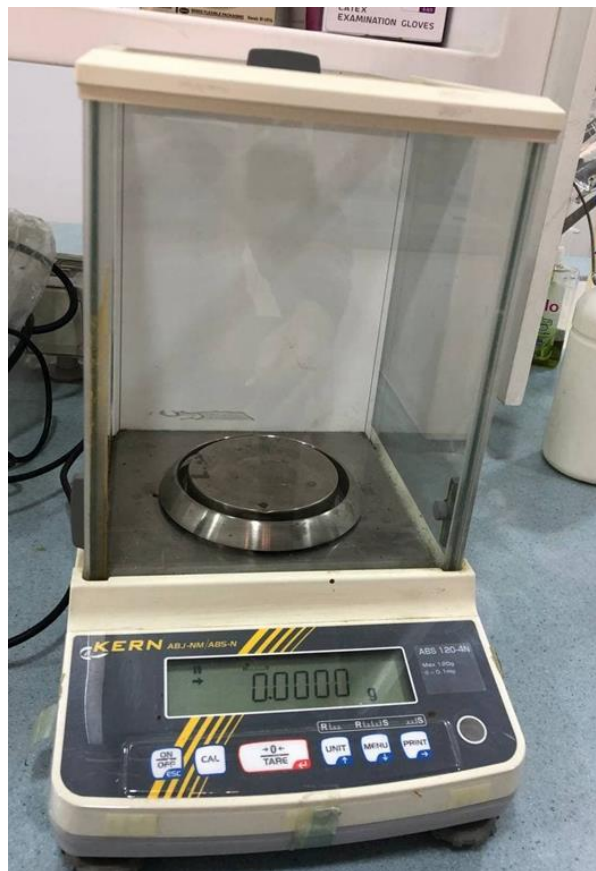


Figure 3.12 Electronic balance

3.6. TEST PARAMETERS

Some parameters were considered for conducting the wear test including sliding distance, temperature, time, sliding speed, and load. Table 3.4 consists of the values of the variable test factors were proposed for this study.

Table 3.4 Wear test parameters used in this study

Starting temperature (°C)	Temperature at the end (°C)	Load (N)	Sliding distance (m)
25	72.4	10, 20, 30	1570, 2356, 3141
75	118.9		
125	173.4		
175	226.3		
225	263.2		

3.7. MECHANICAL TESTS

3.7.1. Hardness Test

Vickers hardness testing equipment was applied to determine the hardness of the disc and both aluminium alloys. The disc and pin specimens were ground and polished before measuring the hardness test using emery paper. To measure the hardness, the pin specimens must be well polished to allow for accurate measurement of impression size. The provided hardness values are an average of five measurements. 20 kg load for pin specimens and 50 kg for disc was applied by hardness machine for a period of 15 sec, and the tests were undertaken at room temperature from a different location, The hardness of the disc is 233 HV that is greater than hardness of Al2024 (140 HV) and Al7075 (189 HV). The macro-Vickers hardness machine is illustrated in Figure 3.13.



Figure 3.13 Vickers hardness machine

3.7.2. Wear Test

For performing tests of dry sliding wear at different temperatures, a pin-on-disc tribo-testing system was applied. The pin of Al2024 and Al7075 was slid against a rotating 2507 duplex stainless steel disc at various starting temperatures such as (25, 75, 125, 175, 225 °C) with sliding distances of (1570, 2356, and 3141 *m*) and under standard weights of (10, 20, and 30 *N*), with a fixed sliding speed of 2.6 *m/s*. Acetone is used to thoroughly clean the pins, and hot air is used to dry them, before and following all tests. Then the amount of the mass that have been lost was determined by the use of a digital balance that had 0.0001 *g* resolution. The wear rate due to the volume loss was calculated using Equation 1.

$$W_r = \frac{\Delta W}{\rho} \text{ (mm}^3\text{)} \quad (3.3)$$

where:

(W_r) is the wear due to the volume loss (mm^3).

(ρ) is the tested material density (g/mm^3).

(ΔW) is the wear amount by volume loss (mm^3).

The distance of sliding was found by:

$$S = 2\pi \times r \times RPM \times t \quad (3.4)$$

where:

(S) is the distance of sliding (m).

(r) is the wear track radius (m).

(RPM) is the revolutions per minute.

(t) is the time (min).

The specific wear rate was found by:

$$W_s = \frac{V}{F \cdot S} \quad (3.5)$$

where:

(W_s) is the specific wear rate ($\frac{\text{mm}^3}{N \cdot m}$).

(F) is the normal applied load (N).

(S) is the distance of sliding (m).

(V) is the material volume loss (mm^3).

The sliding speed was found by:

$$v = \frac{S}{t} \quad (3.6)$$

Where:

(v) is the sliding speed (m/s).

(S) is the sliding distance (m).

(t) is the time (sec).

To ensure the repeatability of the measurement data, each test was repeated three times, and an average was taken.

3.7.3. Microstructure Observation

The worn surface of the pin samples was examined utilizing an optical microscope (Carl Zeiss Axiovert 25) and a scanning electron microscope (SEM) type of (inspect F50) for determining mechanism of wear traces after sliding wear experiments. Throughout all of the tests, the microstructure was inspected. The three temperatures of 25, 125, and 225 °C, loads of (10, 20, and 30N), and sliding distances of (1570, 2356, and 3141 m) were utilized for describing the microstructure of the worn pin surface at different temperatures, loads, and sliding distances for each type of Al alloy. The wear parameter values were just mentioned for the rest temperatures employed in this investigation.

CHAPTER FOUR

RESULTS AND DISCUSSION

4.1. INTRODUCTION

As described in chapter 3, dry sliding wear experiments were conducted for Al2024 and Al7075 under different loads, sliding distances and temperatures. The mechanisms and behavior of wear under different examining conditions were assessed. The sliding speed was maintained constant at 2.6 m/s during the duration of the tests. The subsequent sections provide a detailed presentation of the experiments' findings.

4.2. FRICTIONAL HEAT

Frictional heating is simply the transition of frictional energy created during a friction operation. The temperature increase is influenced by internal and extrinsic factors such as material qualities, tribological circumstances, and ambient temperature. Frictional heating occurs when one part is rotated against the other under pressure. One component is constant, whereas the other rotates with a variable velocity of angular. At the beginning of each test, the temperature was kept constant at the specific degree, but it continuously increases with rotating disc material below the pin specimen. For example, for this graph below which (shown in Figure 4.1), the test temperature was fixed 25, 75, 125, 175, 225 °C and started the test, but continued to increase during the test.

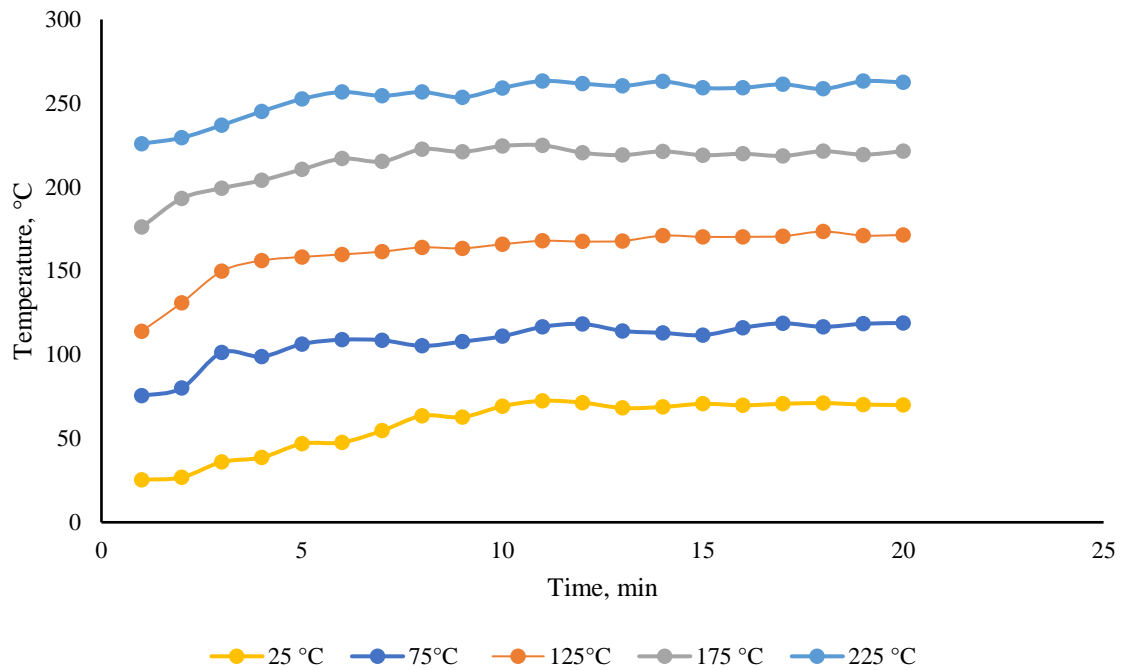


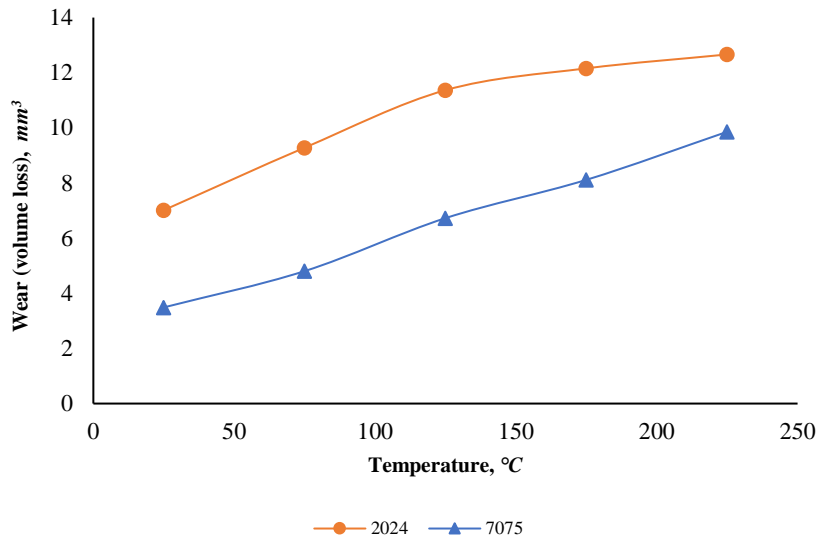
Figure 4.1 Frictional heat during the wear test

4.3. THE IMPORTANT CHARACTERISTICS OF WEAR BEHAVIOR AT DIFFERENT CONDITIONS

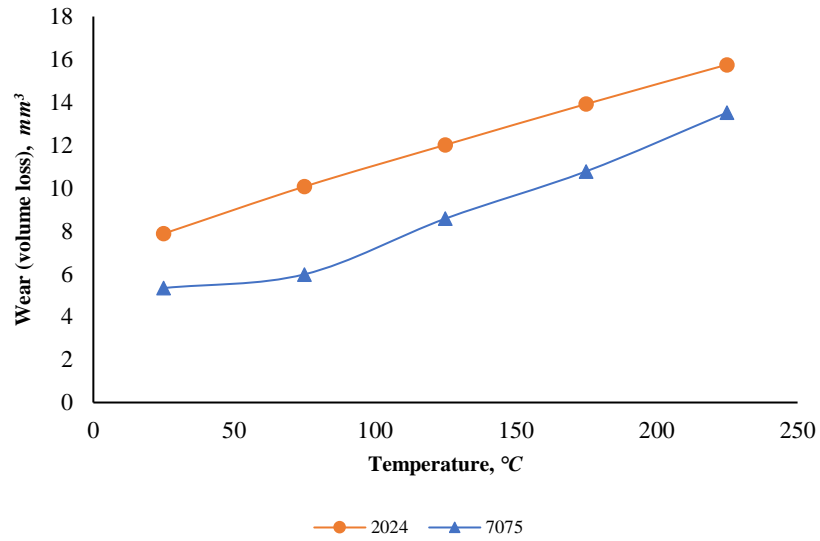
4.3.1. The Effect of Temperature on the Wear

The influence of temperature on the wear due to volume loss of Al2024 and Al7075 is shown in Figure 4.2. A variation in wear could be seen depending on the temperature used for the test. When the temperature increases, the wear also increases, and the quantity of removed material increases considerably. These results support the idea of (Mousavi Abarghouie and Seyed Reihani, 2010; Paulraj and Harichandran, 2020; Aydın, 2021), they suggested that somehow this behavior could be due to a rise in temperature, the alloys in consideration get softer. Adhesive wear is resulted from the soft pin surface interacting with the hard spinning steel disc. Transfer of the alloy to its counterface of steel and increased adhesion offer a rise in wear due to this phenomenon. The specific wear rate will increase as the test temperature increases even though the sliding speed remains constant. According to the idea of (Dabral *et al.*, 2017), this could be because the alloy softens at high

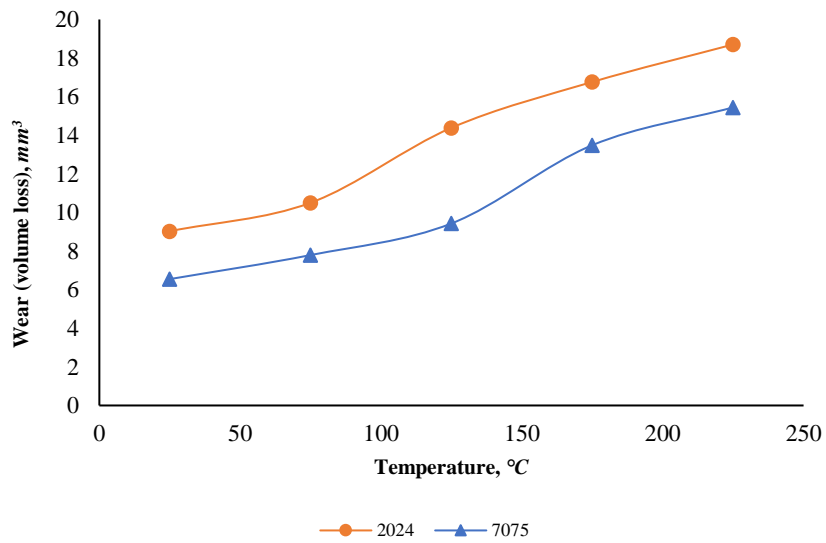
temperatures, causing it less resistant to wear. This makes the specific wear rates increase at high temperatures. According to these findings, the wear due to volume loss and specific wear rate in Al2024 are more than that of Al7075 at any tested temperature. Figure 4.3 to Figure 4.5 show the SEM images of the worn surfaces for aluminium 2024 and aluminium 7075 at different temperatures, while Figure 4.6 depicts images taken using an optical microscope. There were sliding wear scars that showed both mild and severe wear. As mentioned in Chapter 2, mild wear behavior could be defined as fine wear debris and scratches while severe wear could be defined as large wear particles and rough wear marks. As the temperature increases, the wear mechanism gradually shifts to the surface cracks formation. Due to the softening effects of the high operating temperature, the wear mechanism takes a bulk removal form of material in a direction of sliding. Microscopic analysis reveals that wear traces are mostly abrasive, with just small traces of adhesive wear visible. Furthermore, the wear process switched from mild into delamination and subsequently to severe metal wear as the load and temperature continued to increase. (Singh and Alpas, 1995; Wilson and Alpas, 1996; Zhang and Alpast, 1997; Mu *et al.*, 2005) have also reached the same result. Deeper abrasive scratches, grooves, and traces with a bit more adhesive wear can be seen in Al2024 compared to Al7075. This is due to the higher hardness of Al7075.



(a)

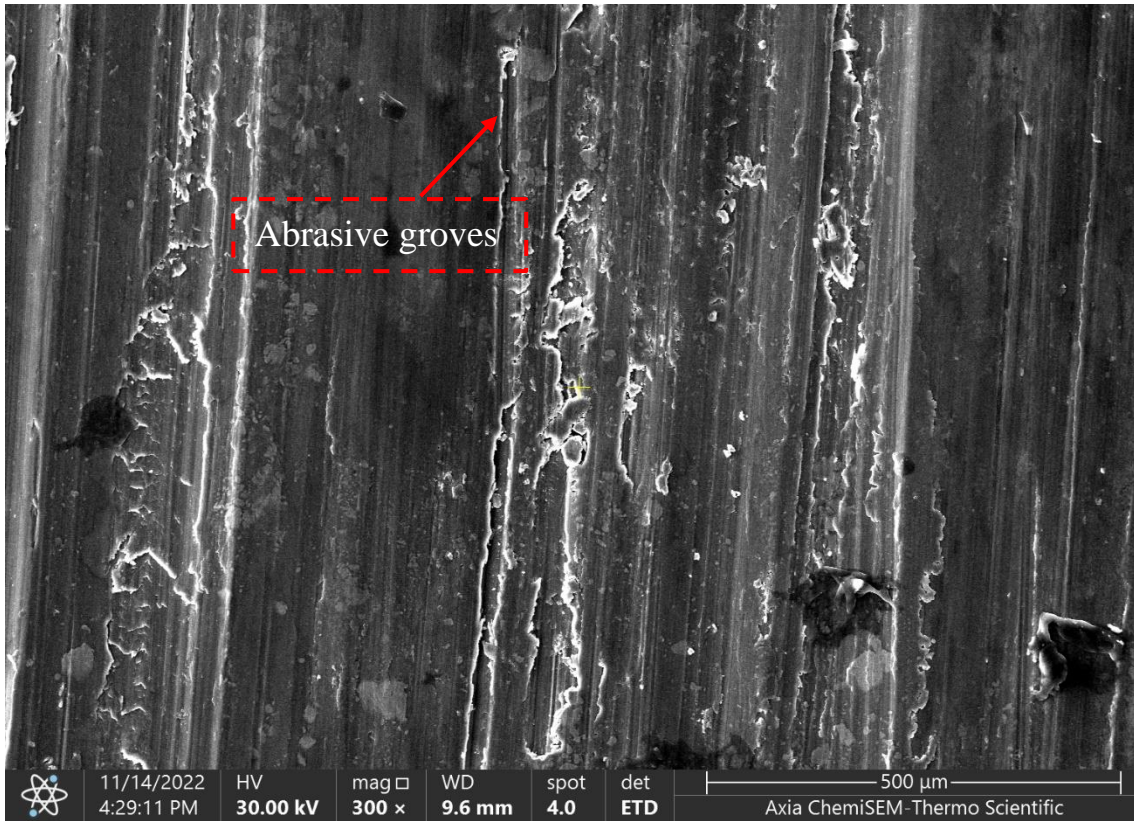


(b)

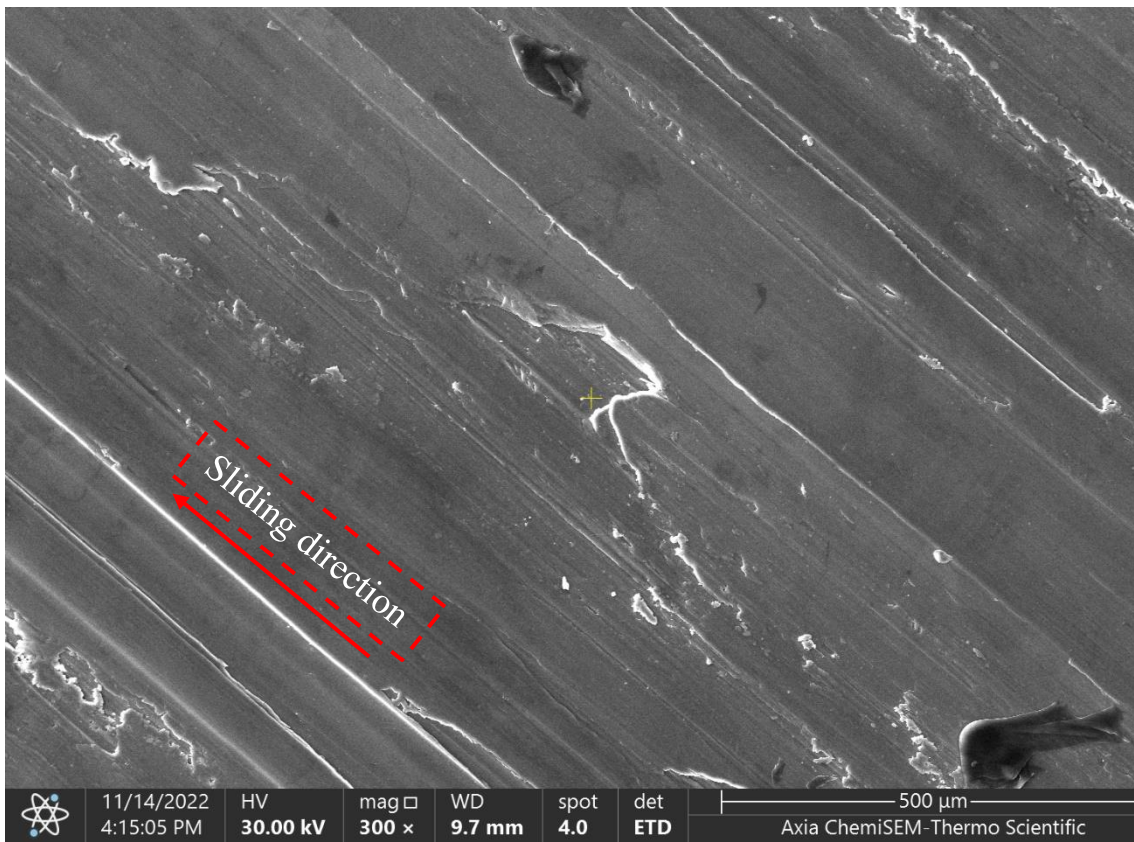


(c)

Figure 4.2 Wear due to volume loss with temperature diagram for (Al2024, Al7075) at, a) 10 N, b) 20 N, c) 30 N.

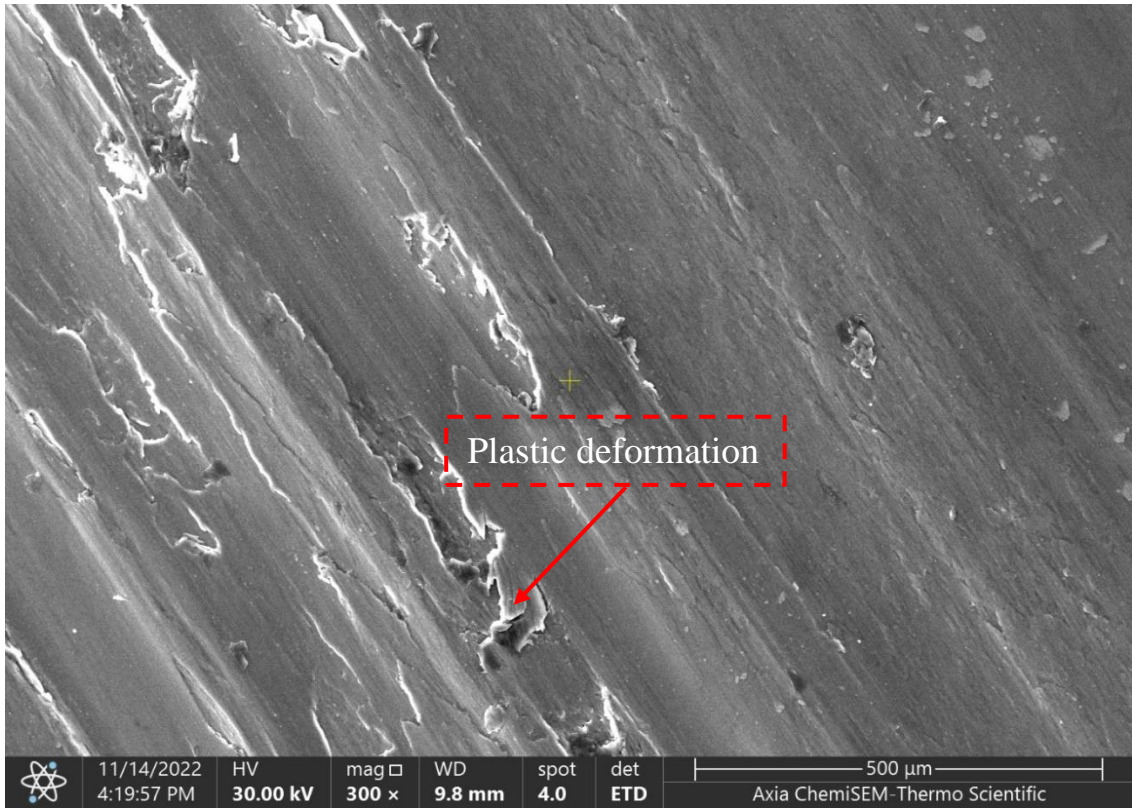


(a)

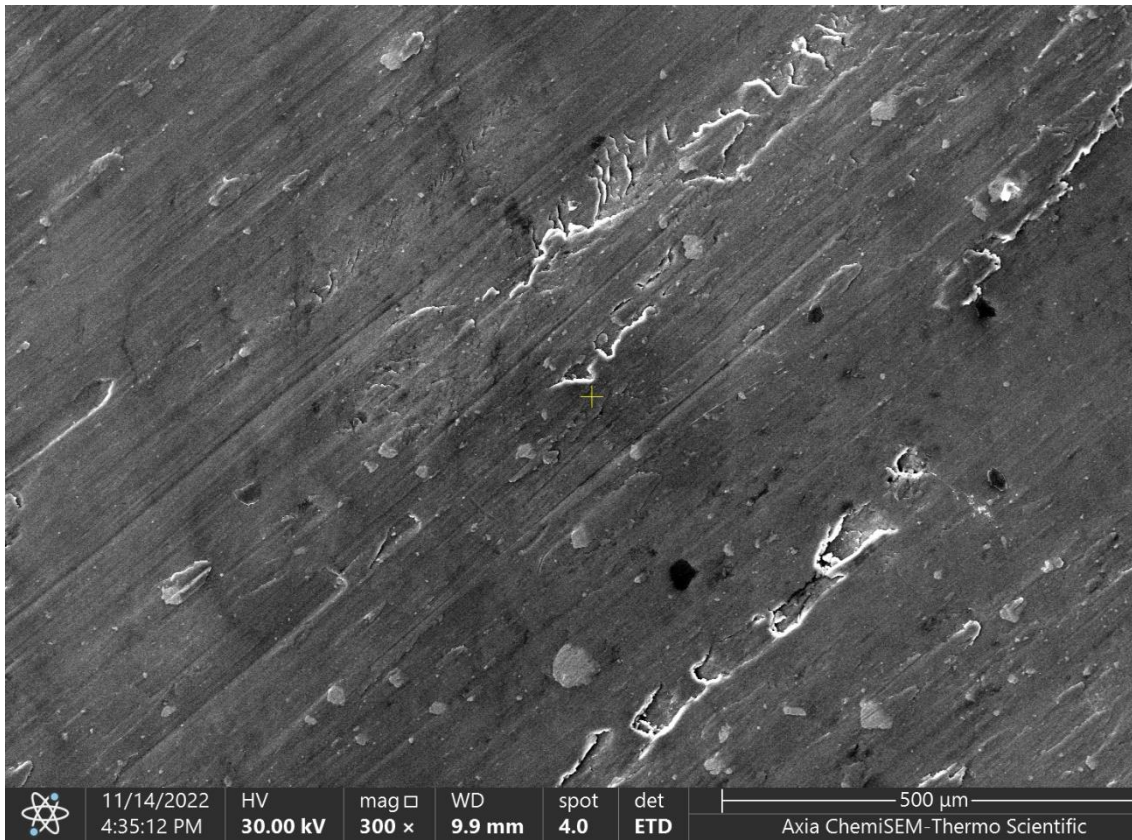


(b)

Figure 4.3 SEM micrograph at constant applied load of 20 N and temperature of 25 °C for, a) Al2024, b) Al7075

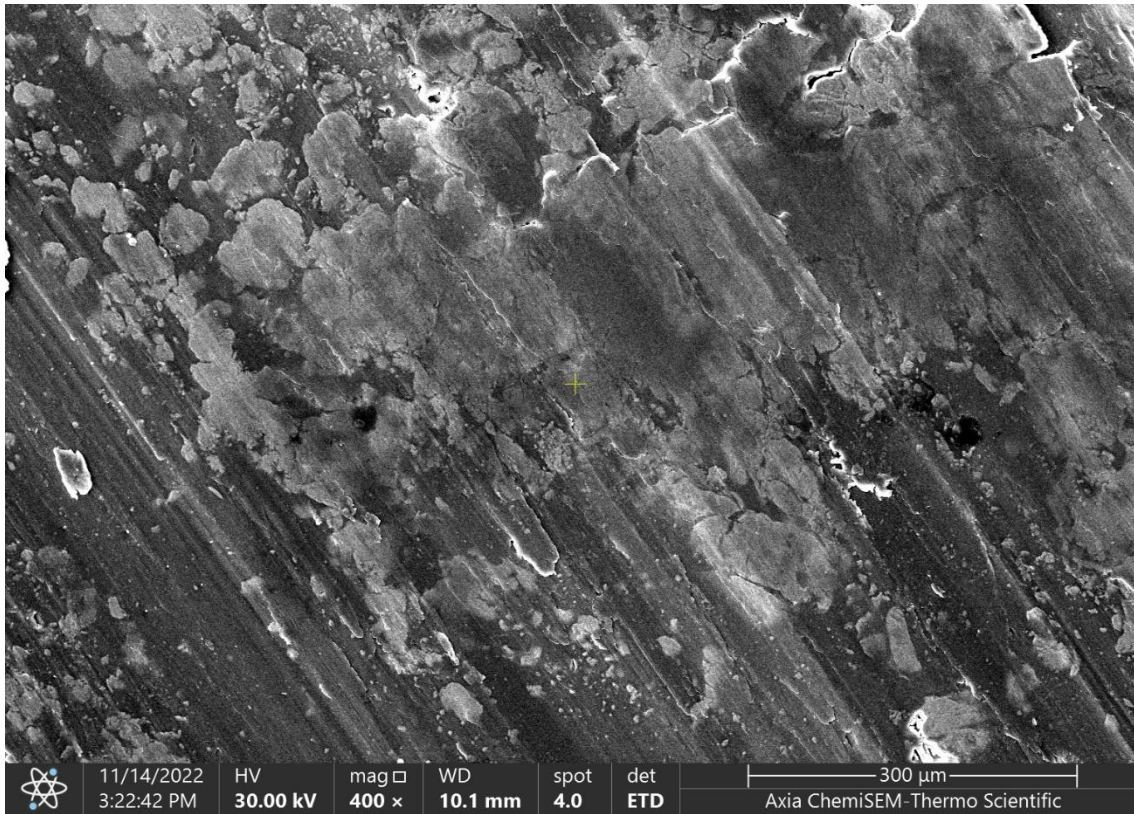


(a)

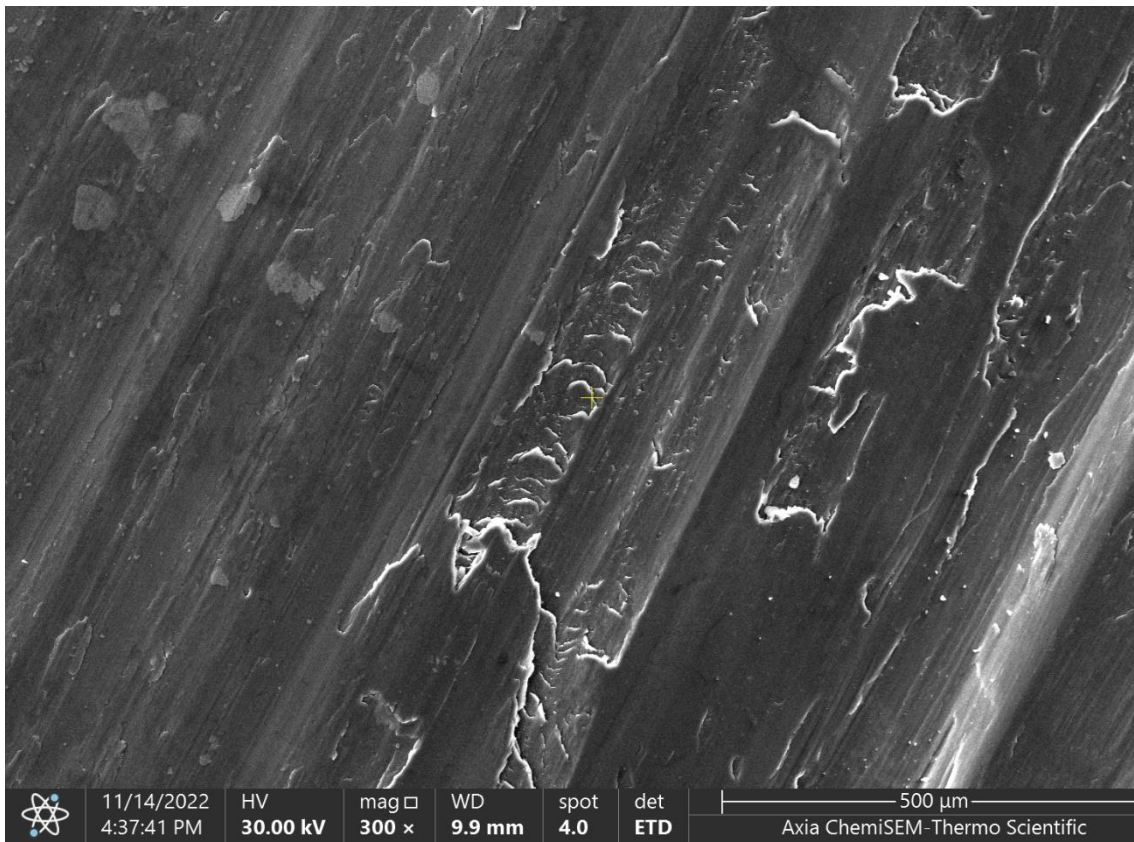


(b)

Figure 4.4 SEM micrograph at constant applied load of 20 N and temperature of 125 °C for, a) Al2024, b) Al7075

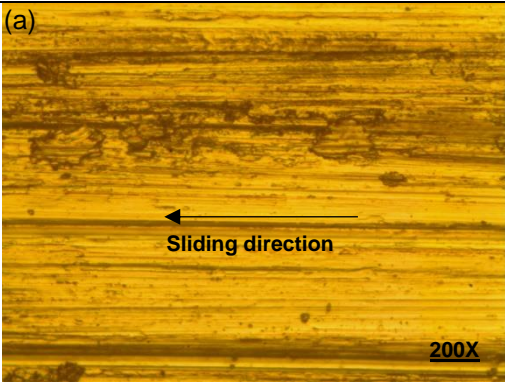
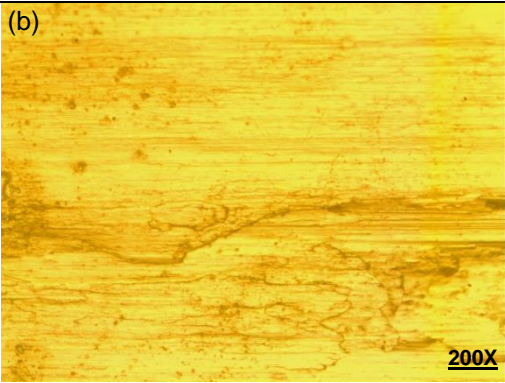
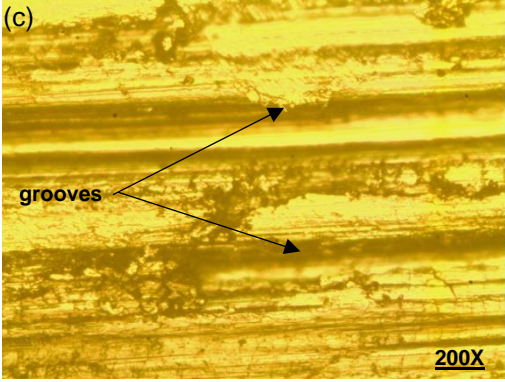
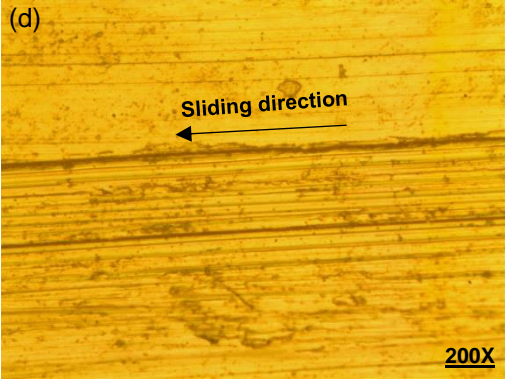
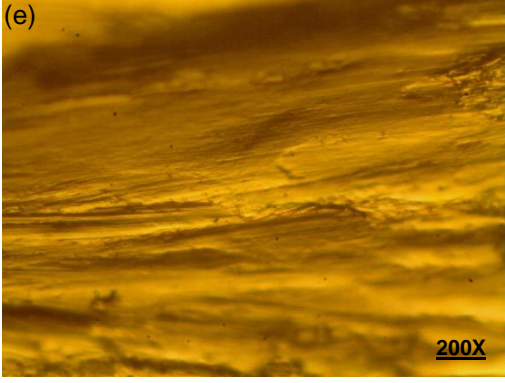
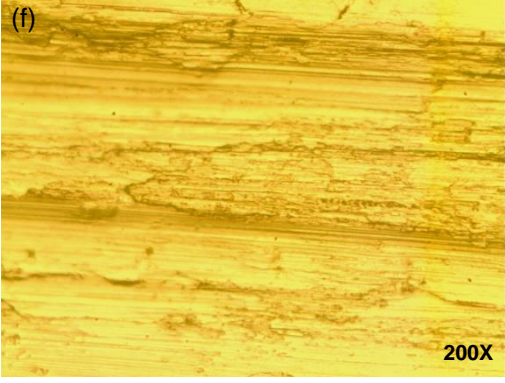


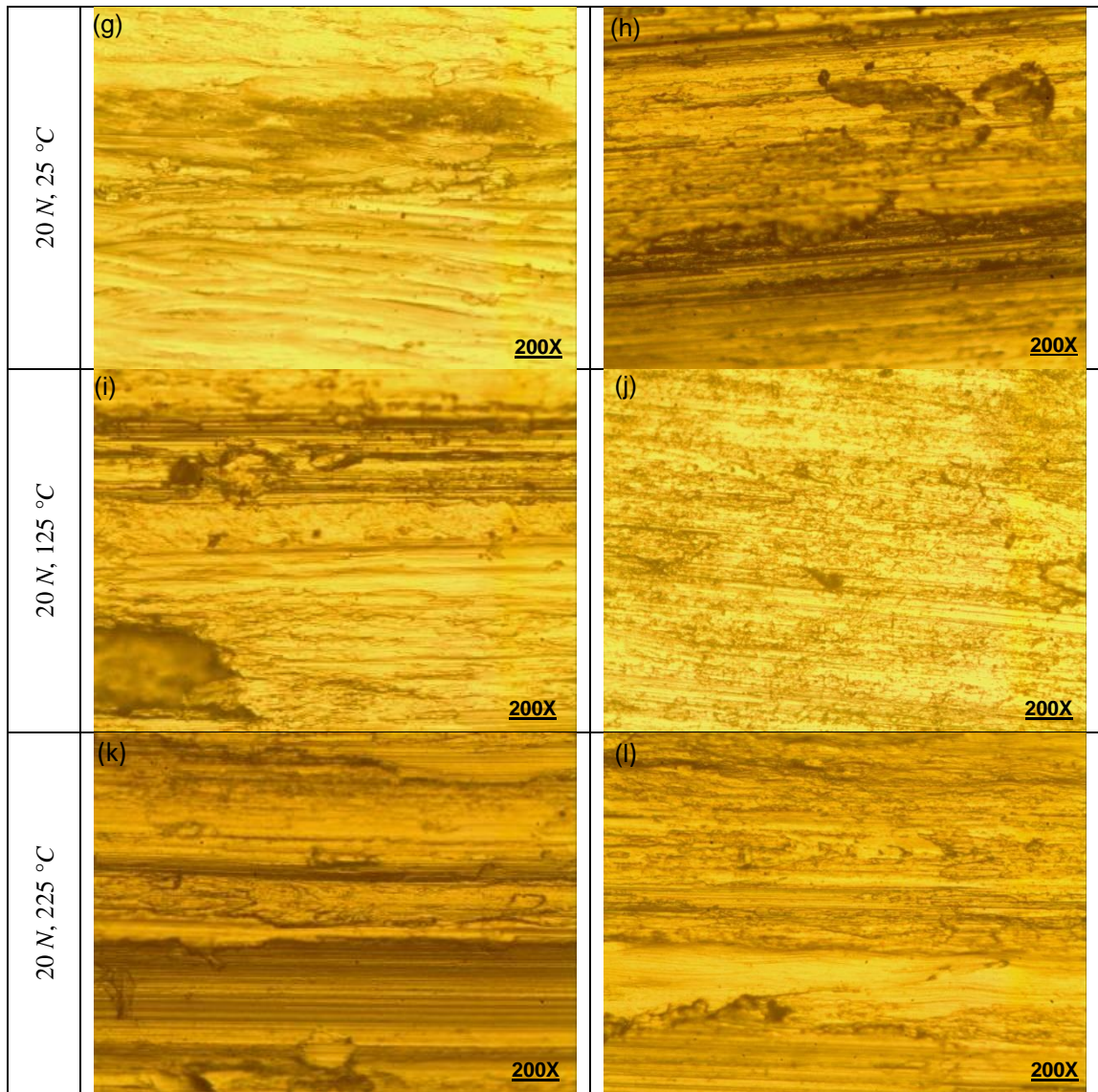
(a)



(b)

Figure 4.5 SEM micrograph at constant applied load of 20 N and temperature of 225 °C for, a) Al2024, b) Al7075

	Al2024	Al7075
10 N, 25 °C	<p>(a)</p> 	<p>(b)</p> 
10 N, 125 °C	<p>(c)</p> 	<p>(d)</p> 
10 N, 225 °C	<p>(e)</p> 	<p>(f)</p> 



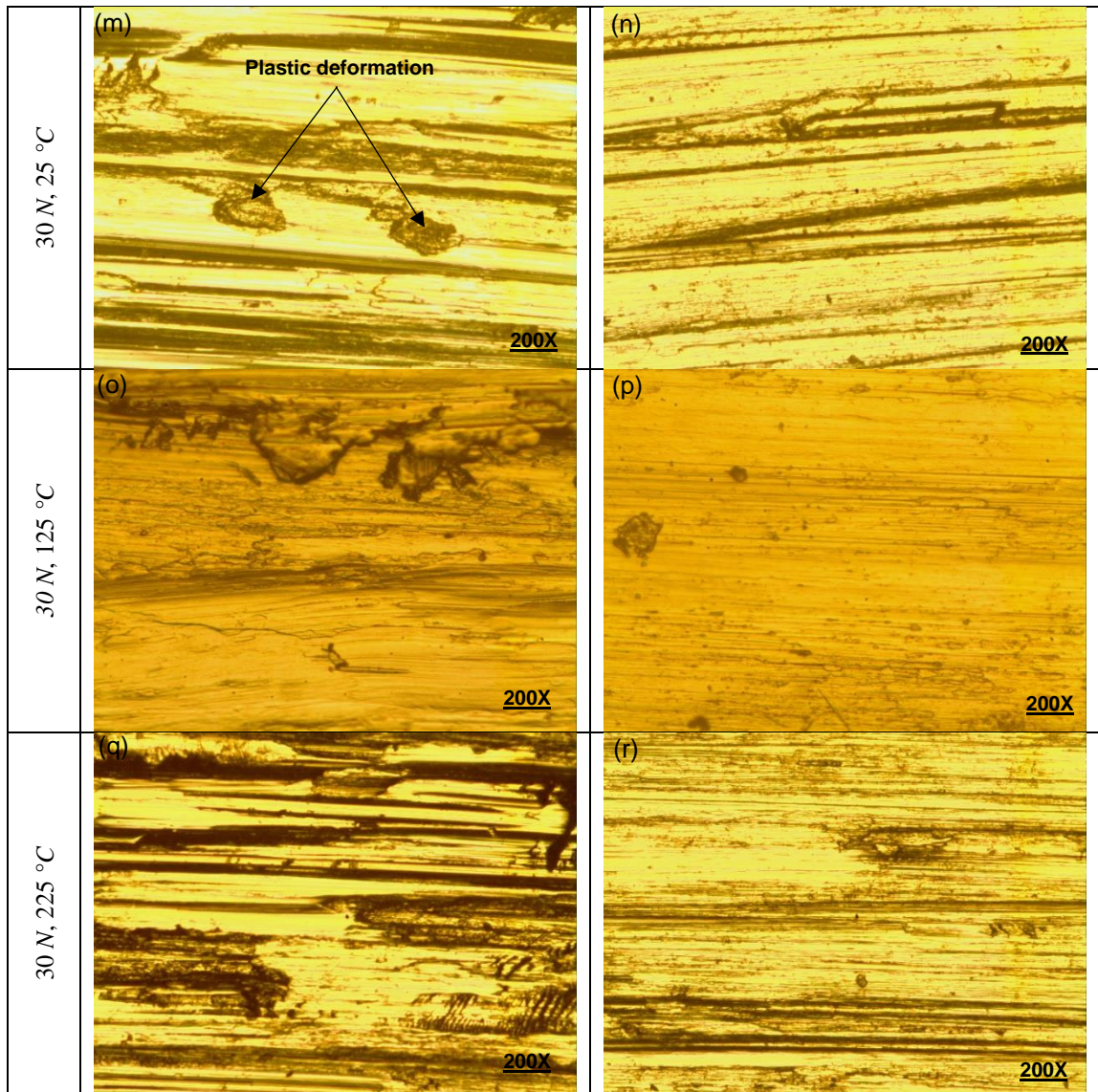


Figure 4.6 Optical micrographs of worn pin surfaces of Al2024 and Al7075 at different loads and temperatures

4.3.2. The Effect of Applied Loads on the Wear

The wear due to volume loss is mainly influenced by the quantity of load applied during the wear testing procedure. It can be explained from the experiments when the load is increased at a certain temperature while the other factors such as sliding distance and sliding speed are fixed, the wear due to volume loss increases as illustrated in Figure 4.7. These findings support the ideas of (Kumar *et al.*, 2013), that is because, at higher loads aluminium alloy and counterface material have more asperity contact points, which increases their ability to interact and connect. Increasing the load at a fixed sliding distance causes a decrease in the specific wear rate (shown in Figure 4.8). As (Kathiresan and Sornakumar, 2010) mentioned, it is because of the alloy's work hardening which occurs when it is exposed to larger loads. As illustrated in SEM findings (Figure 4.9 to Figure 4.11) and microstructure test results in Figure 4.6, the surface of the pin specimens during dry wear at 125 °C and different applied loads revealed different wear mechanisms. The worn surface evolved and formed cracks when the load was increased. In load of 30 N, as seen in Figure 4.11, a significant wear track appeared on pin surfaces. Wear has created deep and significant grooves in the surface.

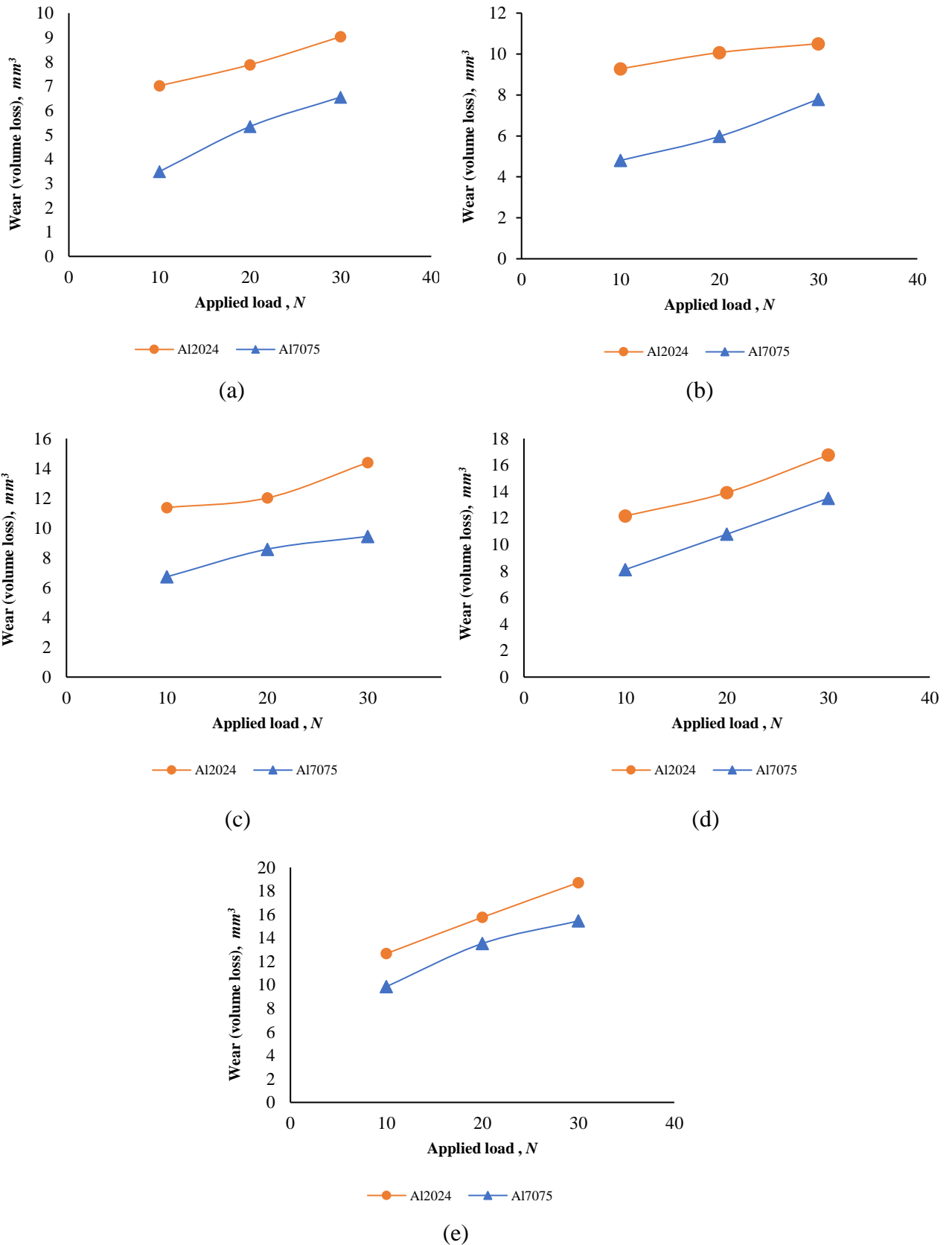
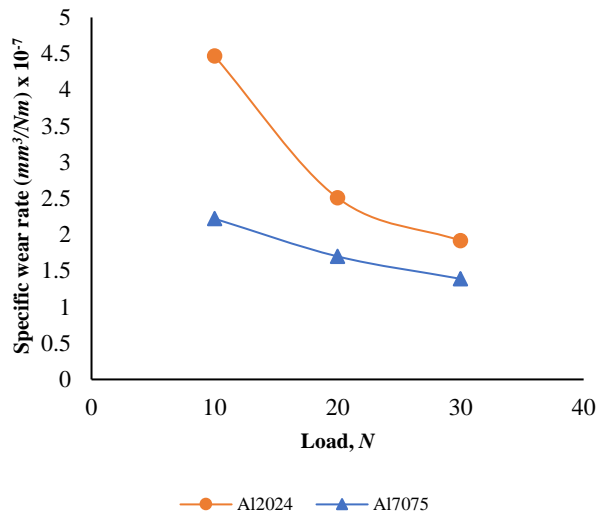
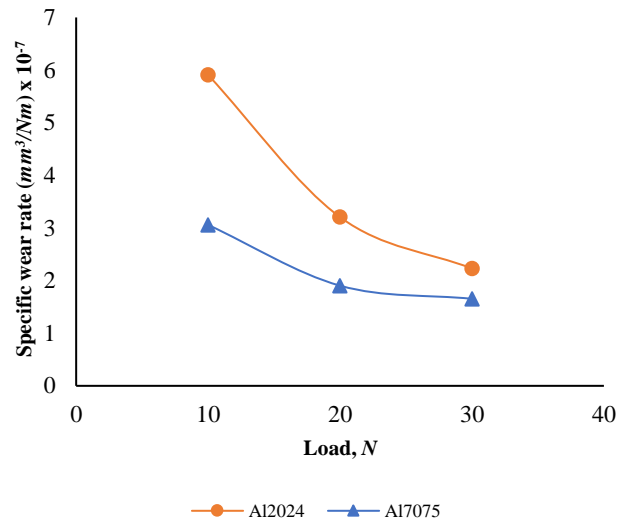


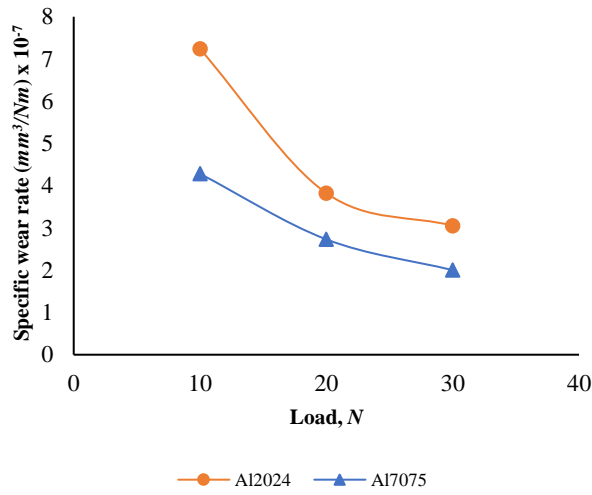
Figure 4.7 Wear due to volume loss with applied load diagram for (Al2024, Al7075) at temperature, a) 25 $^{\circ}C$, b) 75 $^{\circ}C$, c) 125 $^{\circ}C$, d) 175 $^{\circ}C$, e) 225 $^{\circ}C$



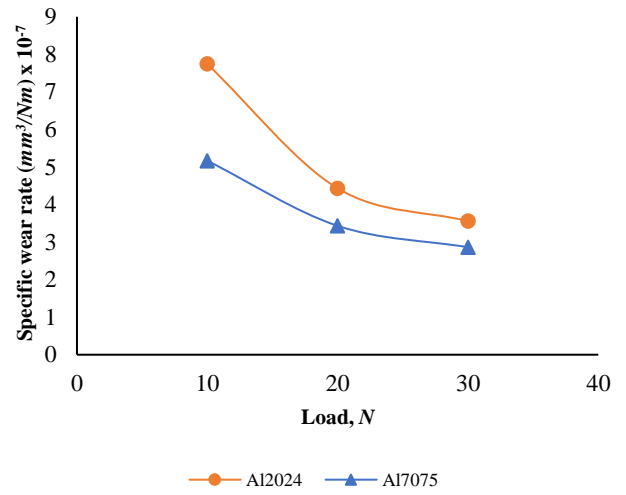
(a)



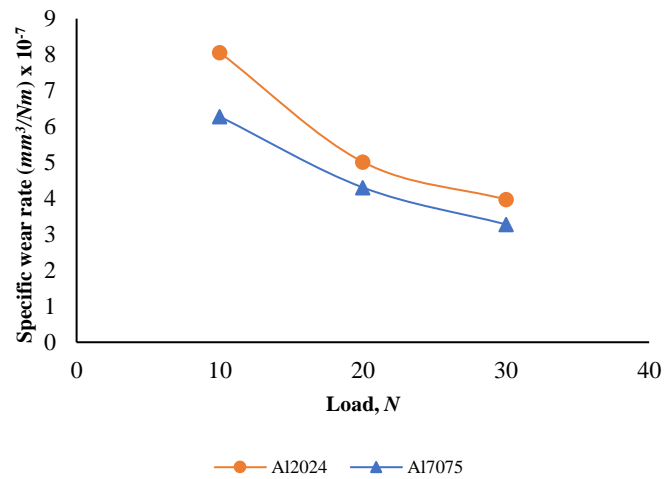
(b)



(c)

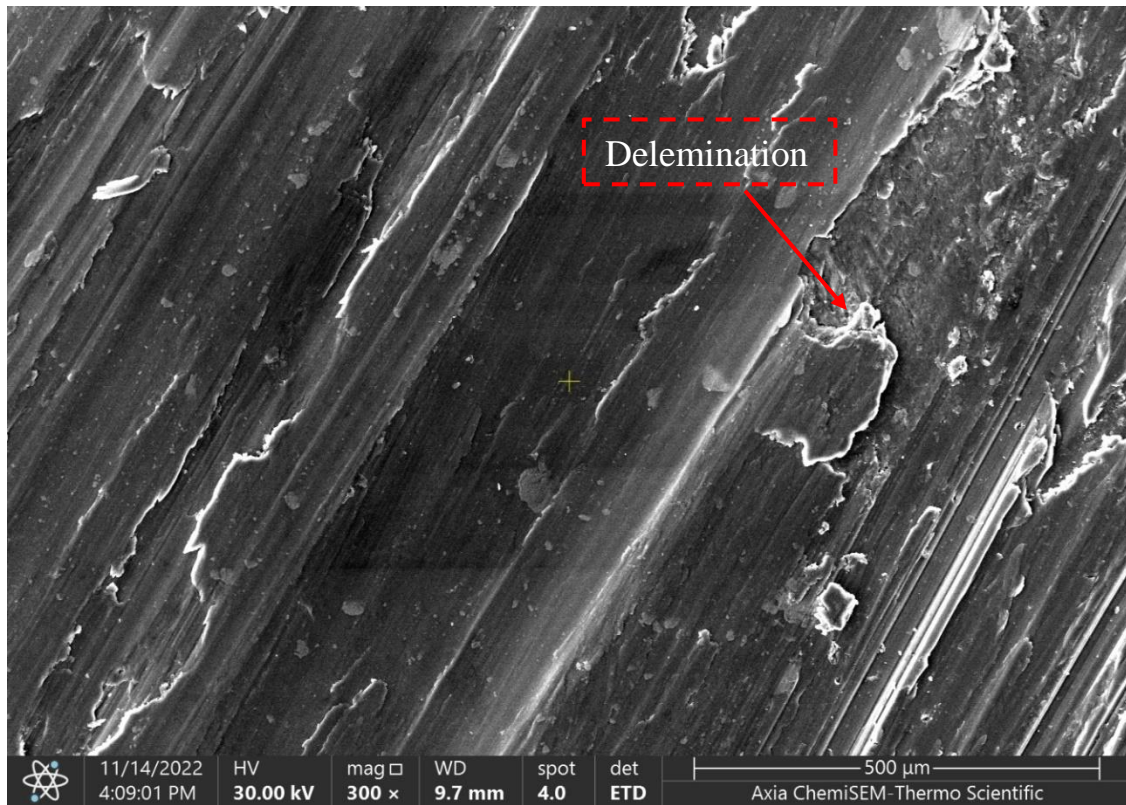


(d)



(e)

Figure 4.8 Specific wear rate with Load diagram for (Al2024, Al7075) at temperature, a) 25 °C, b) 75 °C, c) 125 °C, d) 175 °C, e) 225 °C.

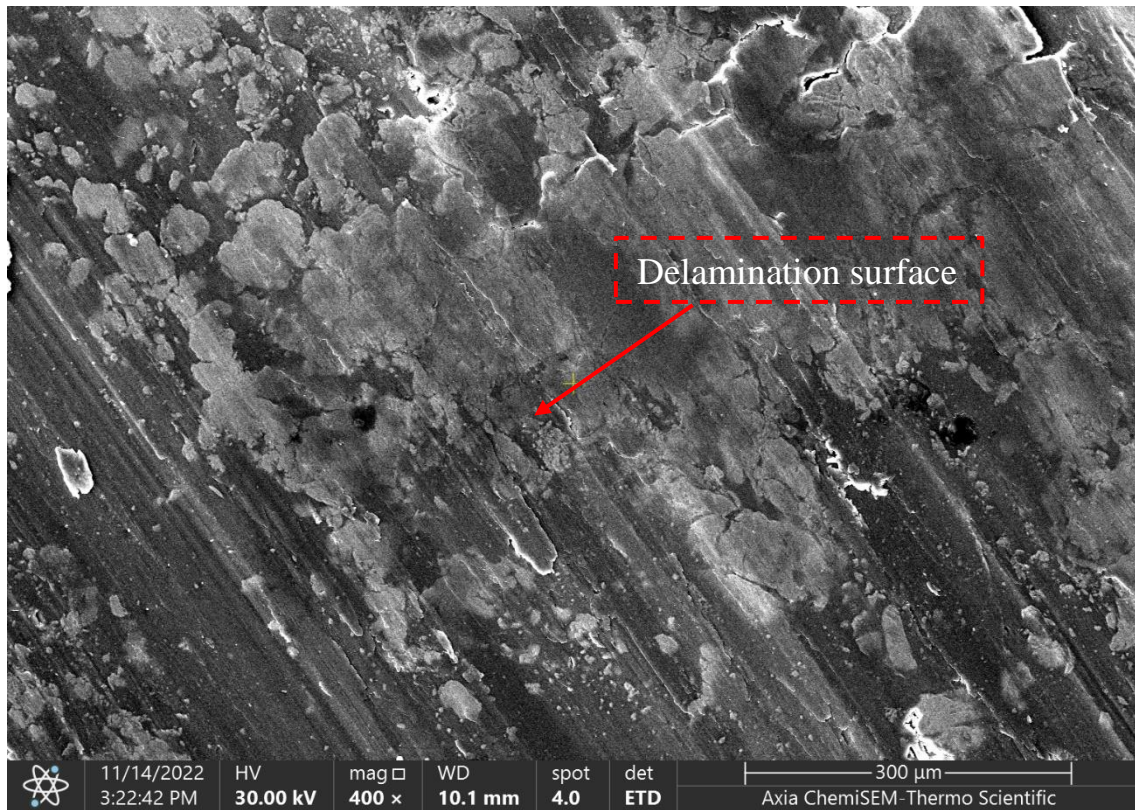


(a)

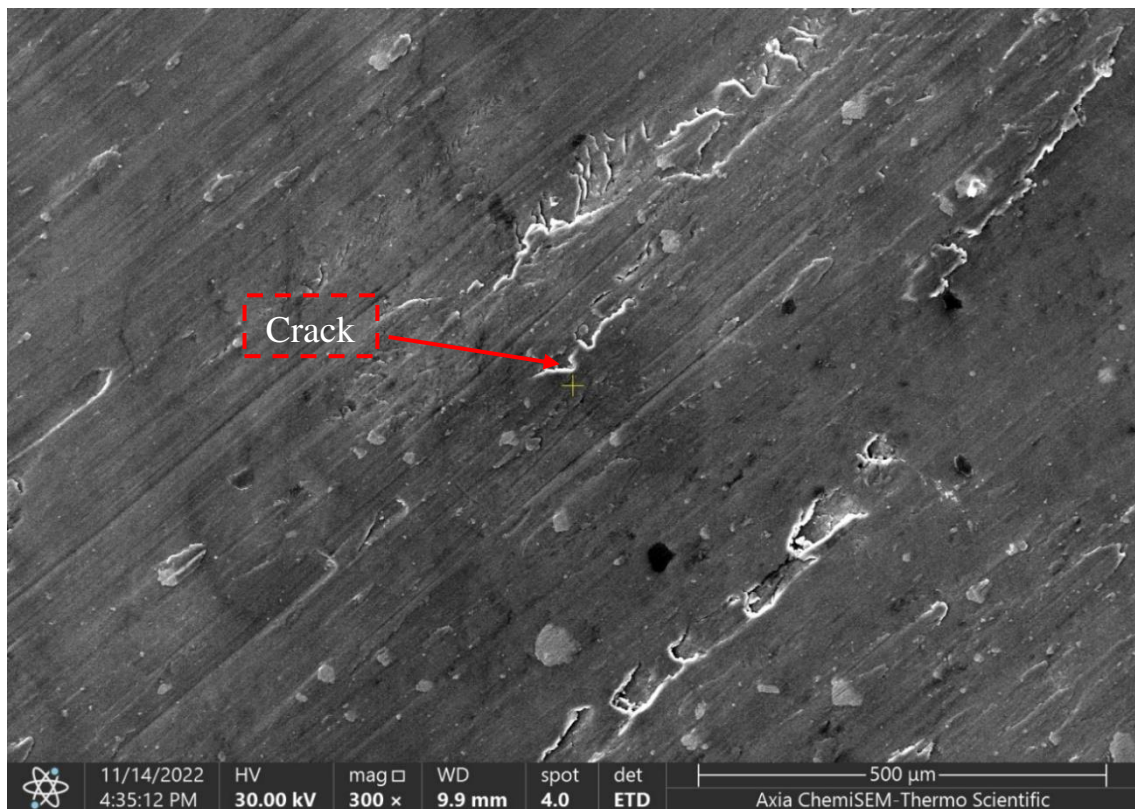


(b)

Figure 4.9 SEM micrograph at a temperature of 125 °C and applied load of 10 N for, a) Al2024, b) Al7075

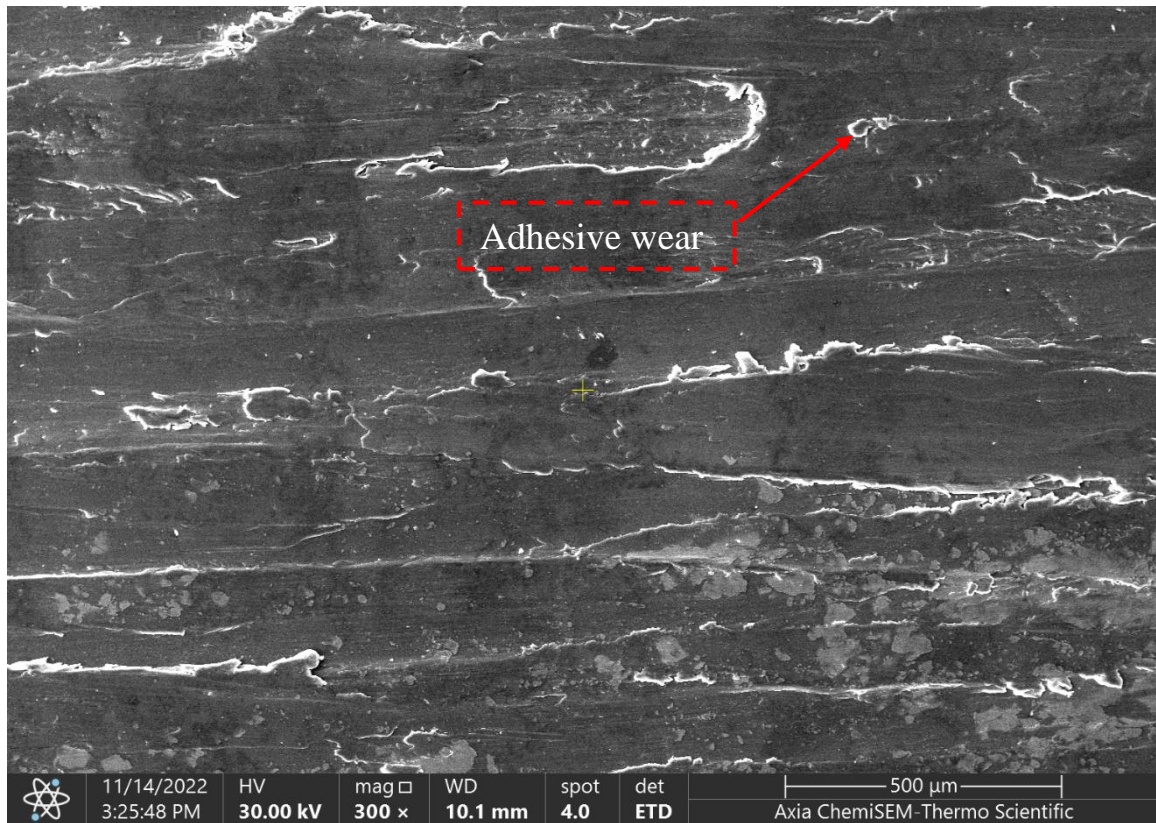


(a)

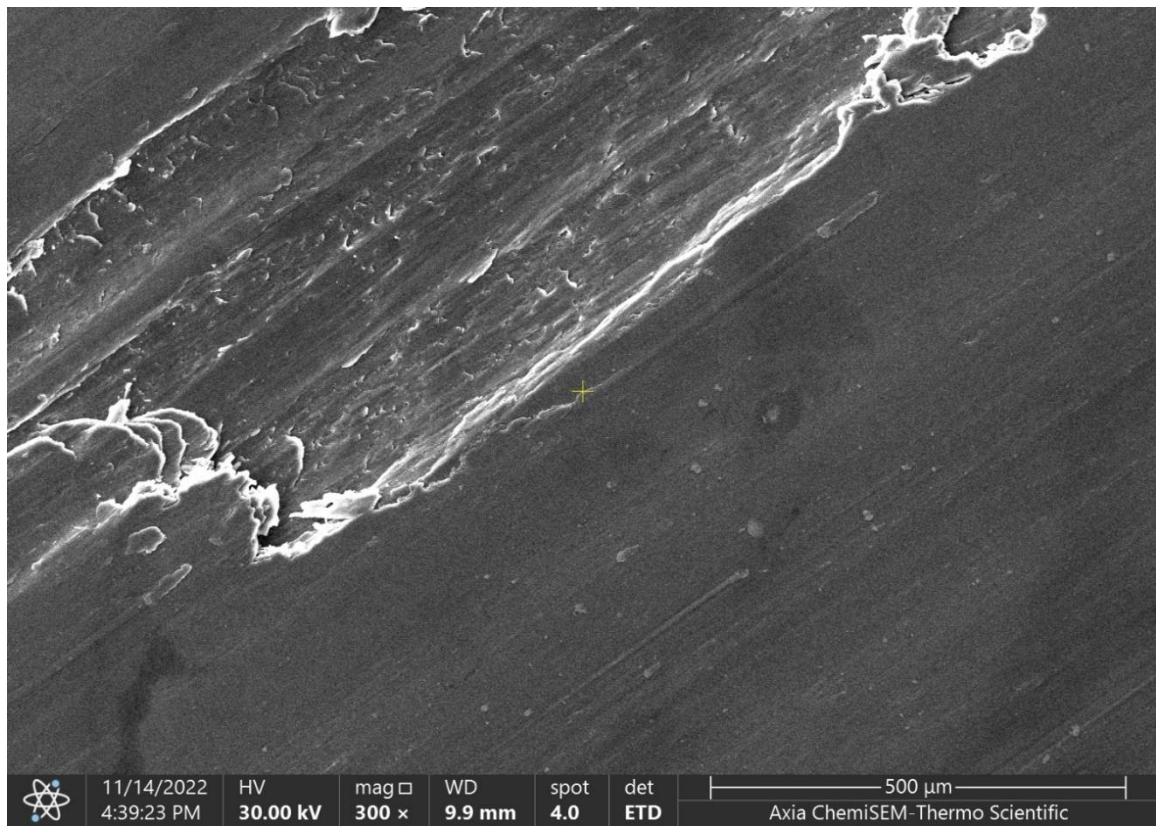


(b)

Figure 4.10 SEM micrograph at a temperature of 125 °C and applied load of 20 N for, a) Al2024, b) Al7075



(a)



(b)

Figure 4.11 SEM micrograph at a temperature of 125 °C and applied load of 30 N for, a) Al2024, b) Al7075

4.3.3. The Effect of Sliding Distance on the Wear

As described in Chapter 3, three different sliding distances, namely 1570, 2356, and 3141 *m*, were employed to explore the impact of sliding distances on the wear behavior of Al2024 and Al7075. It's worth to mentioning that the sliding speed was kept constant at 2.6 *m/s*. The data from this study is shown in Figure 4.12. The wear due to volume loss is significantly increased as a distance of sliding rises from 1570 *m* to 2356 *m*. In addition, with a rise in the sliding distance at any temperature it was seen that the wear in both alloys increased considerably, and that rise in wear was accompanied by a rise in temperature. The wear value reaches its peak while the distance of sliding was 3141 *m* and the temperature is 225 °C. Furthermore, owing to a friction and efficient contact, the initial temperature gradually increases at a fixed load and with increasing sliding distance. Further increase in sliding distance causes higher volume loss, these findings are agreed with (Muratoglu and Aksoy, 2000; Rao *et al.*, 2009; Siddesh and Ravindranath, 2014; Lee *et al.*, 1992). SEM results (Figure 4.13 to Figure 4.15) showing a worn area of alloys at different sliding distances. Sliding causes material to become smooth, with some material which is displaced in the direction of sliding. The worn surface exhibited similar processes such as abrasion and delamination with some cracks in the surface. As the sliding distance is increased, more material was displaced in the surface and more debris was created. The wear due to volume loss is more for Al2024 than Al7075 because of the higher hardness of Al7075 when comparing with Al2024.

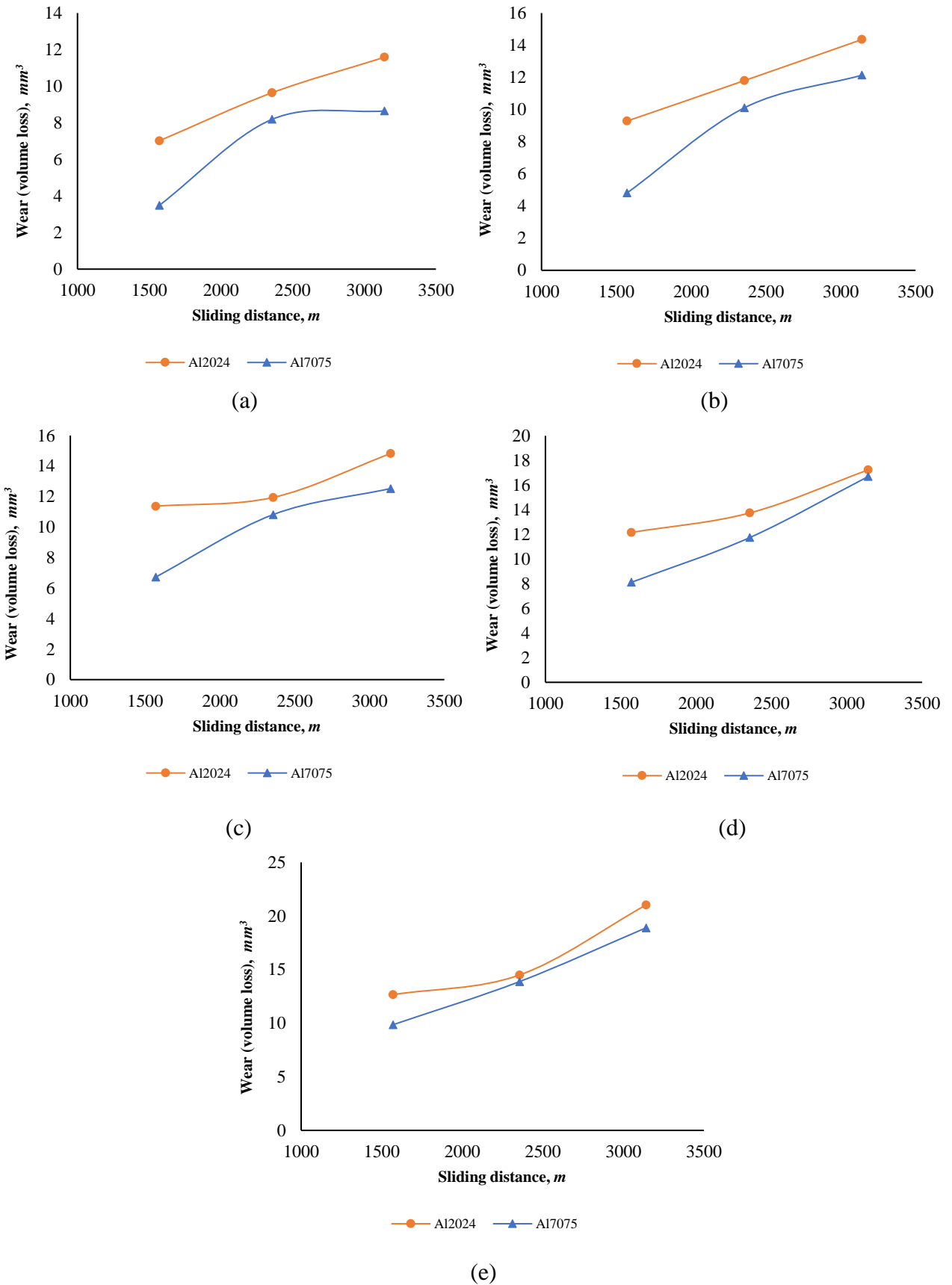
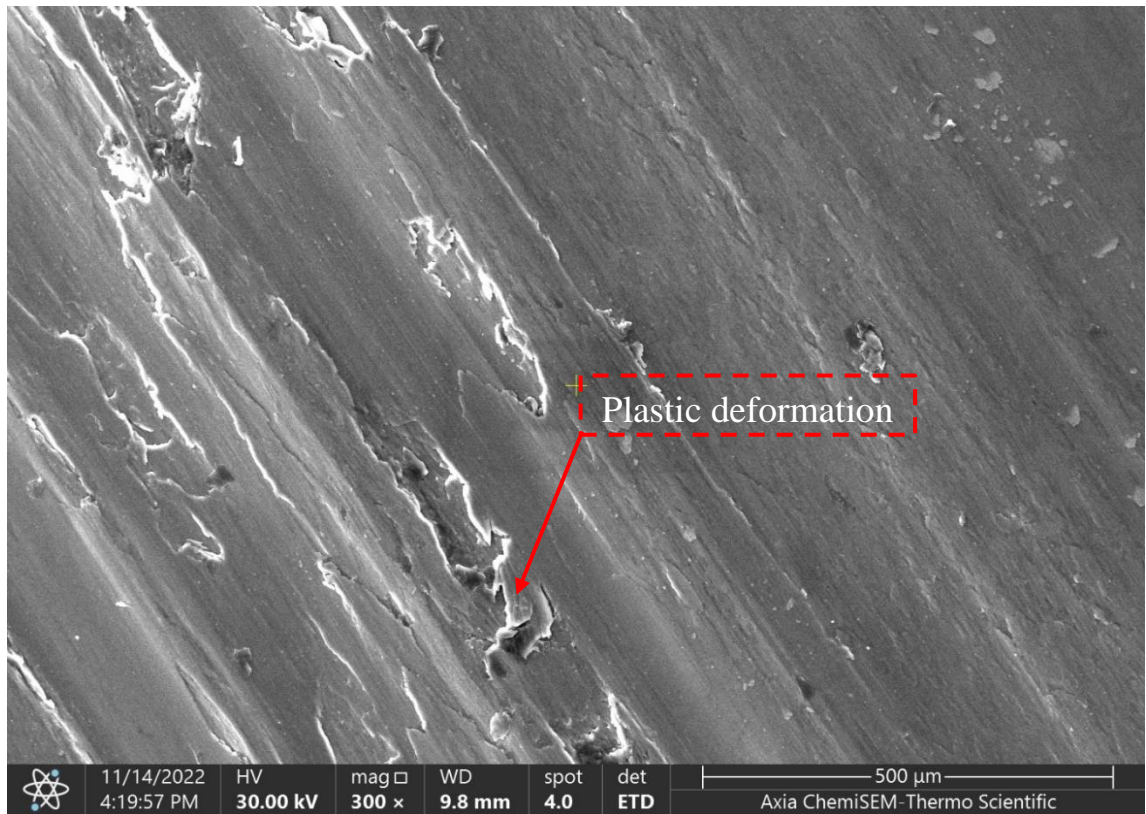
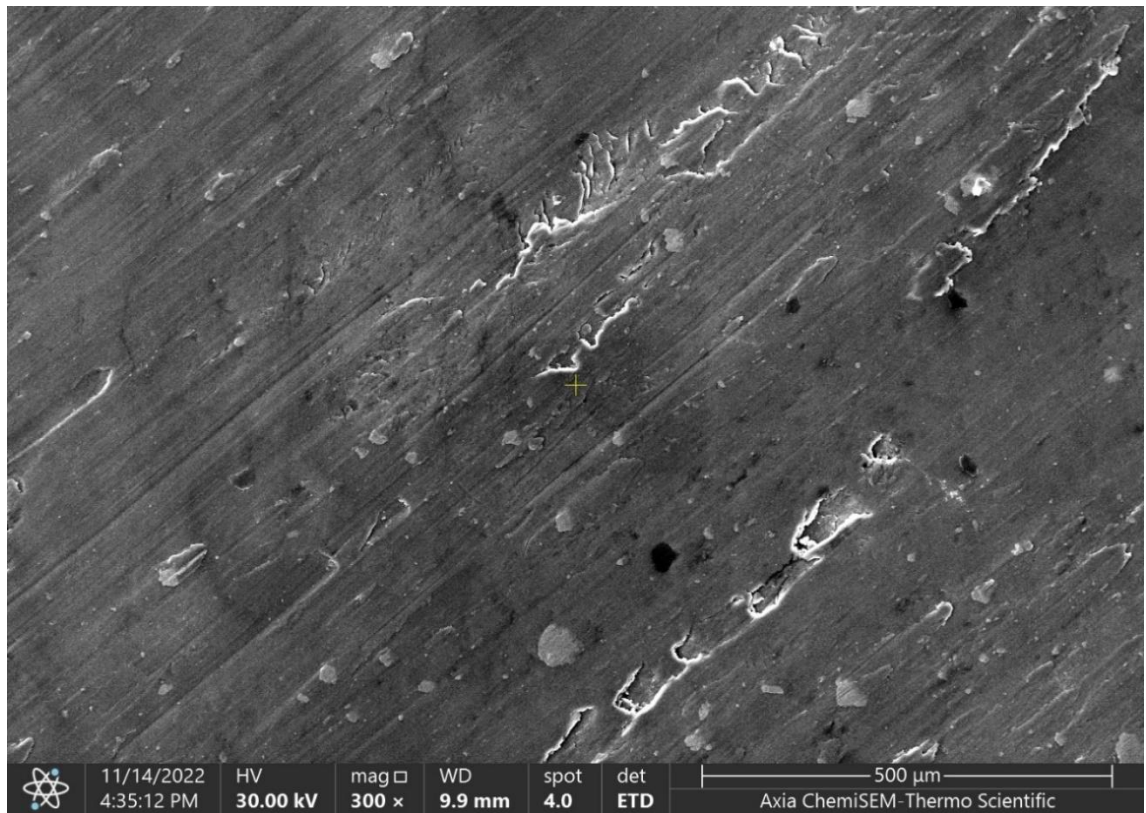


Figure 4.12 Wear due to volume loss with sliding distance diagram for (Al2024, Al7075) at temperature, a) 25 °C, b) 75 °C, c) 125 °C, d) 175 °C, e) 225 °C.

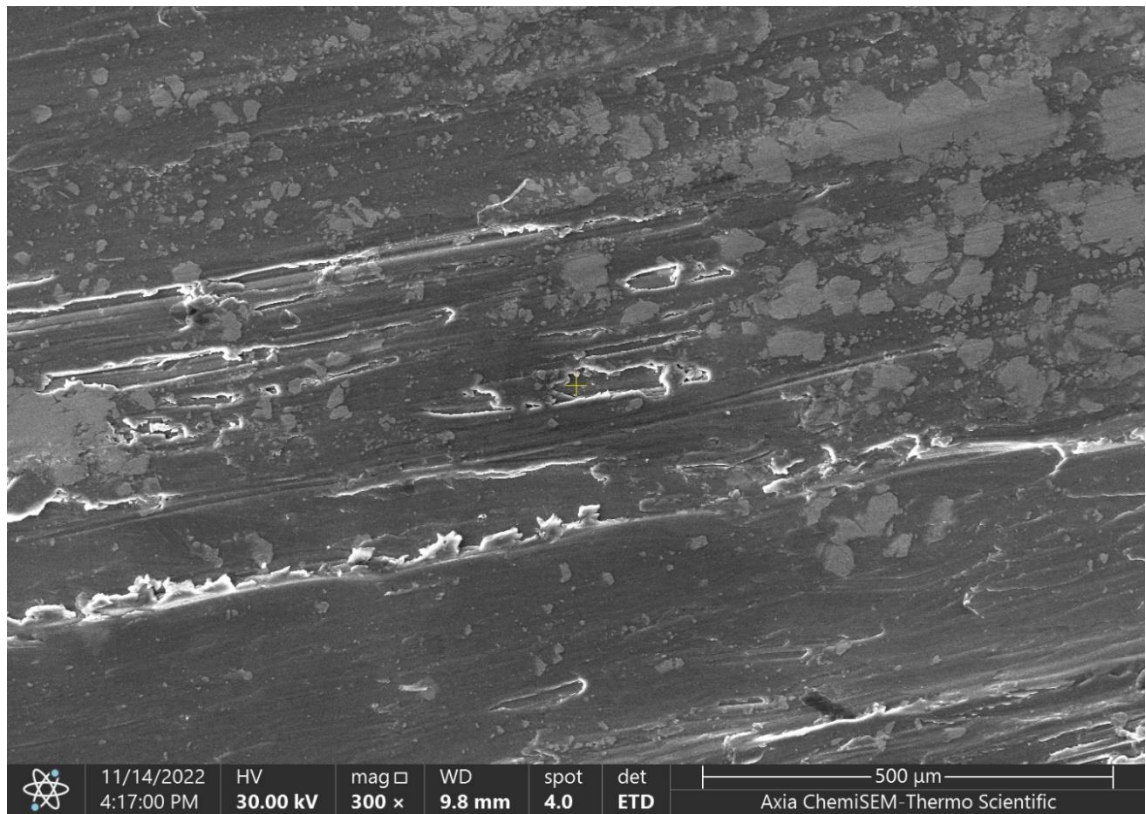


(a)

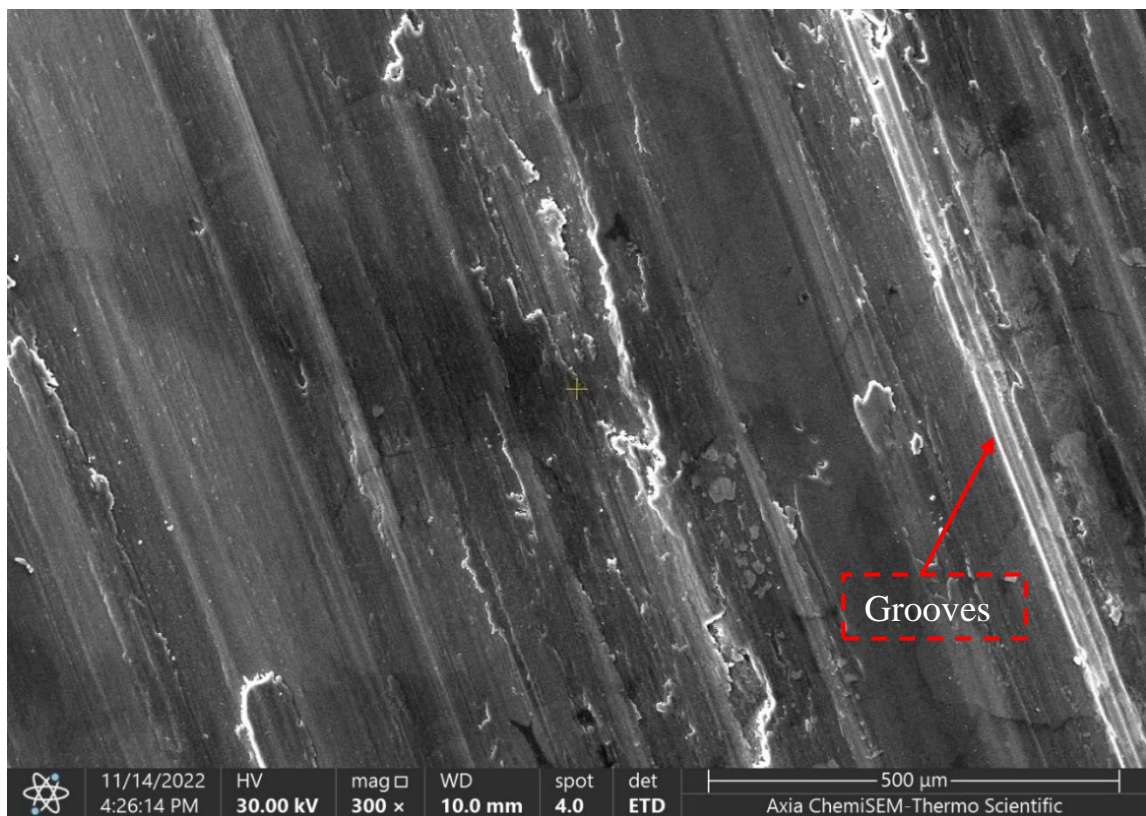


(b)

Figure 4.13 SEM micrograph at sliding distances of 1570 *m* for, a) Al2024, b) Al7075

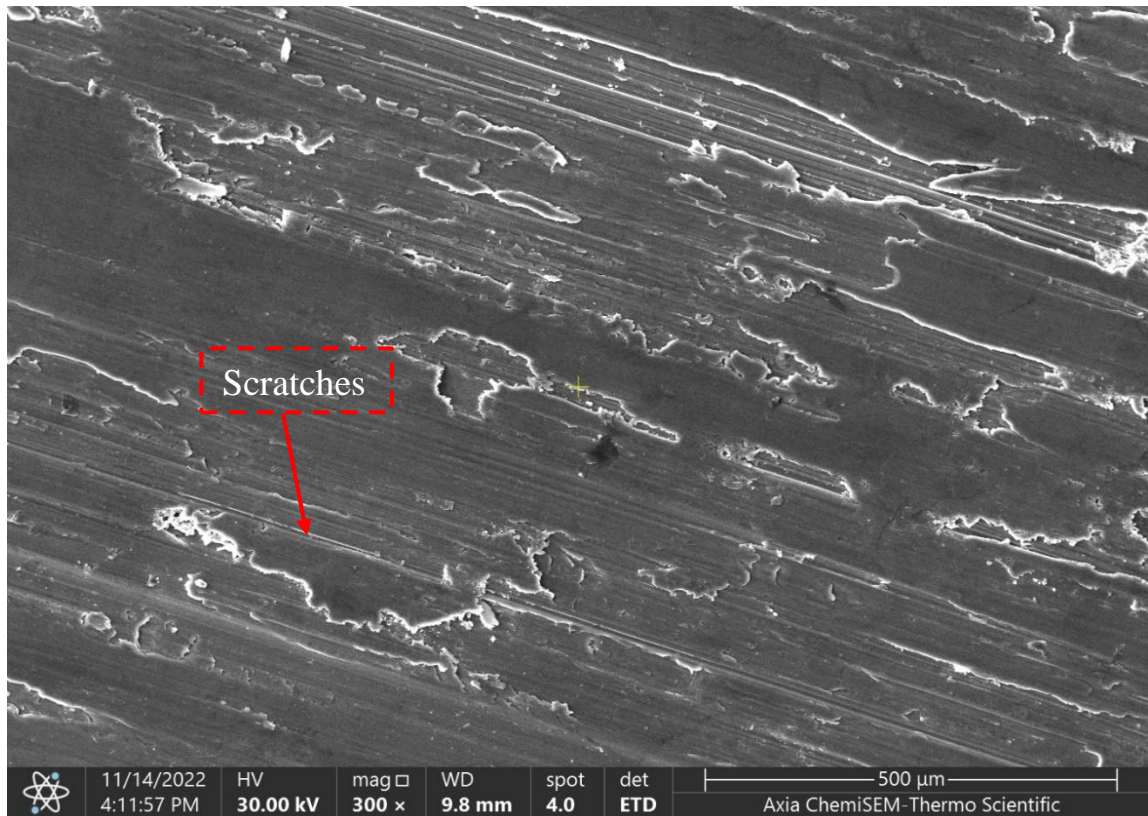


(a)

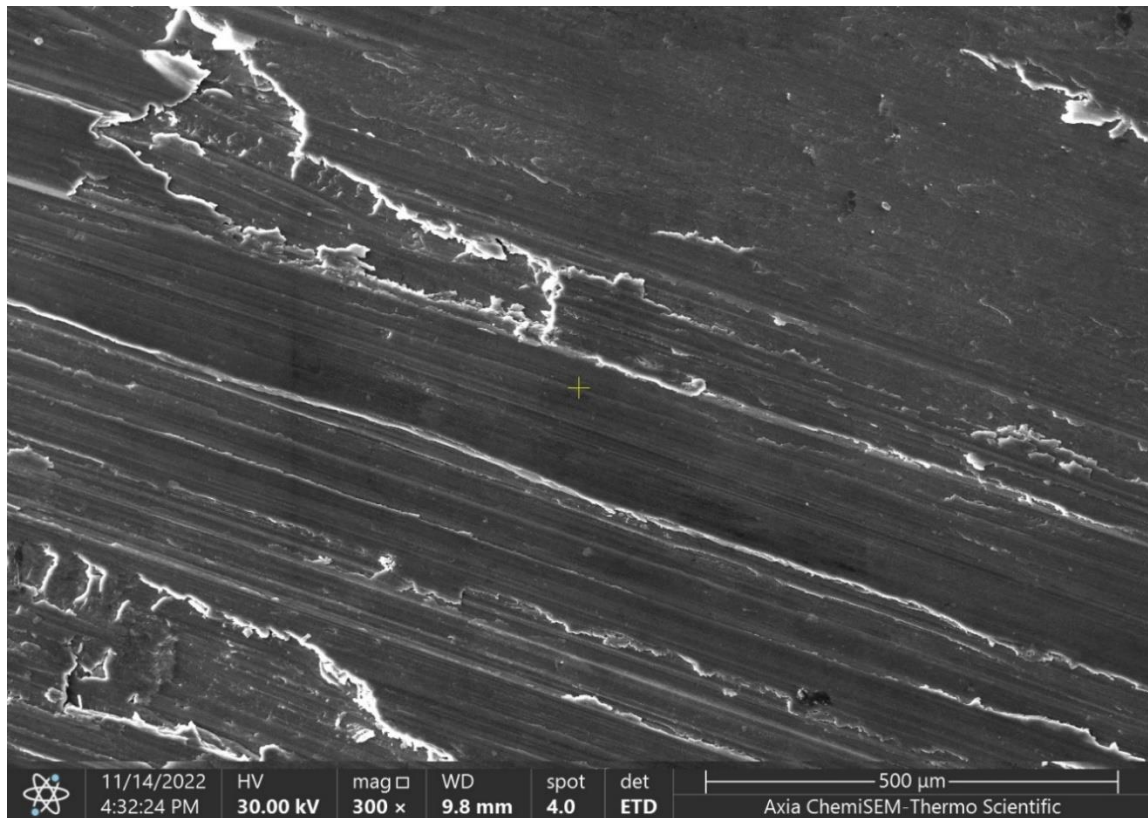


(b)

Figure 4.14 SEM micrograph at sliding distances of 2356 m for, a) Al2024, b) Al7075



(a)



(b)

Figure 4.15 SEM micrograph at sliding distances of 3141 *m* for, a) Al2024, b) Al7075

CHAPTER FIVE

CONCLUSIONS AND RECOMMENDATIONS

5.1. CONCLUSIONS

The primary aim of this work was to investigate the wear behavior of dry sliding of Al2024 and Al7075 at different temperatures, loads and sliding distances. For this purpose, the high temperature testing equipment of pin-on-disc wear was utilized. The following are the findings of this research.

- It was clear that increasing load leads to a rise in wear (volume loss) because the asperity contacts between pin specimens of Al2024 and Al7075 and counterface material increase at higher loads.
- It was found that the amount of material removal and wear debris significantly increases the wear with increase of test temperature at constant sliding speed, load, and time because at elevated temperatures these alloys gradually get softer during the test.
- When the load is increased, the specific wear rate decreases. In addition, by enhancing temperature, the specific wear rate increases.
- As the load and temperature increased, the wear process alerted from moderate to high metal wear. Deep and large grooves were noticed for severe wear. Additionally, it was observed that some material from the pin specimen had been removed and was stuck to the disc surface. Larger and deeper scratches are produced on the surface of Al2024 specimen than Al7075.
- The relation between the sliding distance and wear due to volume loss is directly proportional. Increasing the sliding distance results in a rise in wear for both Al alloys.
- The specific wear rate and wear due to volume loss of Al2024 is more than that of Al7075 in the same test conditions. The higher hardness

value of Al7075 comparing with that of Al2024 causes a lower wear and higher wear resistance in Al7075.

5.2. RECOMMENDATIONS FOR FUTURE WORK

The following suggestions have been identified for future work:

- Different materials or another aluminium alloy series can be used to examine the wear test at elevated temperature, and other disc materials as counterparts can be used instead of AISI 2507.
- Using different tempered Al alloy.
- Using wet conditions for wear tests instead of dry sliding wear tests.
- Performing the surface roughness test for the pin tests after the wear test.
- Using force sensor to measure frictional force.
- More broadly, research is also needed to understand the material removal and the subsurface of the worn samples; a transverse section of worn surfaces will provide us with a solid idea of this.

REFERENCES

Archard, J., 1953. Contact and Rubbing of Flat surfaces. *Journal of Applied Physics*, 24(8), pp.981-988. doi: 10.1063/1.1721448.

Arslan, E. *et al.* (2009) 'High Temperature Wear Behavior of Aluminium Oxide Layers Produced by AC Micro Arc Oxidation', *Surface and Coatings Technology*, 204(6–7), pp. 829–833. doi: 10.1016/j.surfcoat.2009.09.057.

Aydın, F. (2021) 'Investigation of Elevated Temperature Wear Behavior of Al2024-BN Composites using Statistical Technique's, *Journal of Materials Engineering and Performance*, 30(11), pp. 8560–8578. doi: 10.1007/s11665-021-06011-9.

Basavarajappa, S. *et al.* (2006) 'Dry sliding Wear Behavior of Al 2219/SiC Metal Matrix Composite's, *Materials Science- Poland*, 24(2 I), pp. 357–366.

Benedyk, J.C., 2010. International Temper Designation Systems for Wrought Aluminum Alloys. *Light metal age*, 67, pp.3-6.

Bergsma, S. C. and Kassner, M. E. (1996) 'Strengthening in The New Aluminum Alloy AA 6069', *Materials Science Forum*, 217–222(PART 3), pp. 1801–1806. doi: 10.4028/www.scientific.net/msf.217-222.1801.

Bhaskar, S. (2018) 'Elevated Temperature Wear Behavior of Aluminium Alloy (Al 6061)', *National Conference on Latest Trends in Mechanical Engineering NCLTME-2018 Elevated*, (October).

Bhushan, B. (2013) *Introduction To Tribology*. John Wiley & Sons.

Bhushan, B. (2020) 'Wear Mechanism's, *Modern Tribology Handbook, Two Volume Set*, pp. 303–330. doi: 10.1201/9780849377877-15.

Bowden, F. P. and Brunton, J. H. (1961) 'The Deformation of Solids by Liquid Impact at Supersonic Speed's, *Proceedings of the Royal Society of London*.

Series A. Mathematical and Physical Sciences, 263(1315), pp. 433–450. doi: 10.1098/rspa.1961.0172.

Bowman, W. F. and Stachowiak, G. W. (1996) ‘A Review of Scuffing Model’s, *Tribology Letters*, 2(2), pp. 113–131. doi: 10.1007/BF00160970.

Cayless, R.B.C., 2013. Alloy and Temper Designation Systems for Aluminum and Aluminum Alloys

Dabral, R. *et al.* (2017) ‘Wear Response of Aluminium 6061 Composite Reinforced with Red Mud at Elevated Temperature’, *Tribology in Industry*, 39(3), pp. 391–399. doi: 10.24874/ti.2017.39.03.14.

Das, V. V. and Mohanty, C. P. (2011) ‘Tribological Studies on Aluminium Alloy’s, *Rozprawa doktorska*. Available at: [http://ethesis.nitrkl.ac.in/2149/1/Tribological_studies_on_Aluminium_alloys\(107MM030_%26_107MM035\).PDF](http://ethesis.nitrkl.ac.in/2149/1/Tribological_studies_on_Aluminium_alloys(107MM030_%26_107MM035).PDF).

Davis, J. R. and Park, M. (2001) ‘Alloying: Understanding the Basics’.

Dębiński, M. and Brezáni, M., 2018. Fretting Wear as an Example of Destruction of Railway Vehicles Wheelsets. *New Trends in Production Engineering*, 1(1), pp.371-376. doi: 10.2478/ntpe-2018-0046.

Dwivedi, D. K. (2010) ‘Adhesive Wear Behavior of Cast Aluminium-Silicon Alloys: Overview’, *Materials and Design*, 31(5), pp. 2517–2531. doi: 10.1016/j.matdes.2009.11.038.

Dyson, A. (1975) ‘Scuffing - A review’, *Tribology International*, 8(2), pp. 77–87. doi: 10.1016/0301-679X(75)90056-0.

Ellis, E. G. (1965) *Fundamentals of Lubrication, Industrial Lubrication and Tribology*. doi: 10.1108/eb052784.

Engel, P.A. and Ling, F.F., 1978. Impact Wear of Materials. *Journal of Applied Mechanics*, 45(2), p.458. doi: 10.1115/1.3424343.

Eyre, T. S. (1981) 'Wear Mechanism's, *Powder Metallurgy*, 24(2), pp. 57–63. doi: 10.1179/pom.1981.24.2.57.

Finne, I. (1960) 'Erosion of Surface's, *Wear*, 3, pp. 87–103. doi: 10.1016/0043-1648(60)90055-7.

Gee, M. G. and Jones, S. O. (1998) 'Wear Testing Methods and their Relevance to Industrial Wear Problem's, 1997(December 1997), pp. 1–53.

Geitner, F. K. and Bloch, H. P. (2012) *Metallurgical Failure Analysis, Machinery Failure Analysis and Troubleshooting*. doi: 10.1016/b978-0-12-386045-3.00002-7.

Gohar, R. and Rahnejat, H., 2018. *Fundamentals of Tribology*. World Scientific.

Gurumoorthy, K. *et al.* (2007) 'Development and Use of Combined Wear Testing Equipment for Evaluating Galling and High Stress Sliding Wear Behavior', *Materials and Design*, 28(3), pp. 987–992. doi: 10.1016/j.matdes.2005.11.018.

Heinz, A. *et al.* (2000) 'Recent Development in Aluminium Alloys for Aerospace Applications', *Materials Science and Engineering A*, 280(1), pp. 102–107. doi: 10.1016/S0921-5093(99)00674-7.

Heymann, F. J. (1969) 'High-Speed Impact between a Liquid Drop and a Solid Surface', *Journal of Applied Physics*, 40(13), pp. 5113–5122. doi: 10.1063/1.1657361.

Immarigeon, J. P. *et al.* (1995) 'Lightweight Materials for Aircraft Applications', *Materials Characterization*, 35(1), pp. 41–67. doi: 10.1016/1044-5803(95)00066-6.

Izumi, T. *et al.* (2018) 'Surface Deteriorations During Scuffing Process of Steel and Analysis of Their Contribution to Wear Using In Situ Synchrotron X-Ray

Diffraction and Optical Observation's, *Tribology Letters*, 66(3), p. 0. doi: 10.1007/s11249-018-1062-6.

Jeyaprakash, N. and Yang, C.H., 2020. Friction, lubrication, and wear. In *Tribology in Materials and Manufacturing-Wear, Friction and Lubrication*. IntechOpen.

Kaçar, H. U., Atik, E. and Meriç, C. (2003) 'The Effect of Precipitation-Hardening Conditions on Wear Behaviors at 2024 Aluminium Wrought Alloy', *Journal of Materials Processing Technology*, 142(3), pp. 762–766. doi: 10.1016/S0924-0136(03)00642-3.

Kathiresan, M. and Sornakumar, T. (2010) 'Friction and Wear Studies of Die Cast Aluminium Alloy-Aluminium Oxide-Reinforced Composite's, *Industrial Lubrication and Tribology*, 62(6), pp. 361–371. doi: 10.1108/00368791011076263.

Kato, K. (2014) 'Classification of Wear Mechanisms/Model's, *Wear - Materials, Mechanisms and Practice*, pp. 9–20. doi: 10.1002/9780470017029.ch2.

Kato, K. and Adachi, K., 2000. Wear Mechanisms. In *Modern Tribology Handbook: Volume One: Principles of Tribology* (pp. 273-300). CRC press.

Kaufman, J. G. (2000) *Introduction to Aluminum Alloys and Tempers*. ASM International.

Kaufman, J.G. and Rooy, E.L., 2004. *Aluminum alloy castings: properties, processes, and applications*. Asm International.

Kosel, T.H., 1992. Solid Particle Erosion. *ASM handbook*, 18, pp.199-213.

Kovaříková, I., Szewczyková, B., Blaškoviš, P., Hodúlová, E. and Lechovič, E., 2009. Study and Characteristic of Abrasive Wear Mechanisms. *Materials Science and Technology*, 1, pp.1-8.

- Kumar, P. R. S. *et al.* (2010) ‘High Temperature Sliding Wear Behavior of Press-extruded AA6061 / Fly Ash Composite’, *Materials Science and Engineering A*, 527, pp. 1501–1509. doi: 10.1016/j.msea.2009.10.016.
- Kumar, S. *et al.* (2013) ‘Effect of Particle Size on Wear of Particulate Reinforced Aluminium Alloy Composites at Elevated Temperature’s, *Journal of Materials Engineering and Performance*, 22(11), pp. 3550–3560. doi: 10.1007/s11665-013-0642-8.
- Lee, A. *et al.* (2014) ‘Wear Behavior of Human Enamel Against Lithium Disilicate Glass Ceramic and Type III Gold’, *Journal of Prosthetic Dentistry*, 112(6), pp. 1399–1405. doi: 10.1016/j.prosdent.2014.08.002.
- Lee, C. S. *et al.* (1992) ‘Wear Behavior of Aluminium Matrix Composite Material’s, *Journal of Materials Science*, 27(3), pp. 793–800. doi: 10.1007/BF02403898.
- Li, X. M. and Starink, M. J. (2001) ‘Effect of Compositional Variations on Characteristics of Coarse Intermetallic Particles in Overaged 7000 Aluminium Alloy’s, *Materials Science and Technology*, 17(11), pp. 1324–1328. doi: 10.1179/026708301101509449.
- Ludema, C., K. (1984) ‘A Review of Scuffing and Running-in Surfaces, With Asperities and Oxide’s, *Wear*, 100, pp. 315–331. doi: 10.1016/0043-1648(84)90019-X.
- Martin, A., Martinez, M. A. and Llorca, J. (1996) ‘Wear of Sic-Reinforced Al-Matrix Composites in the Temperature Range 20-200 °C’, *Wear*, 193, pp. 169–179. doi: 10.1016/0043-1648(95)06704-3.
- Martin, A., Llorca, J. and Rodriguez, J. (1999) ‘Temperature Effects on the Wear Behavior of Particulate Reinforced Al-based Composite’s, *Wear*, pp. 615–620. doi: 10.1016/S0043-1648(98)00385-8.

- Mathan Kumar, N., Senthil Kumaran, S. and Kumaraswamidhas, L. A. (2016) 'Wear Behavior of Al 2618 Alloy Reinforced with Si₃N₄, AlN and ZrB₂ in Situ Composites at Elevated Temperature's, *Alexandria Engineering Journal*, 55(1), pp. 19–36. doi: 10.1016/j.aej.2016.01.017.
- Meric, C. (2000) 'Investigation on the Elastic Modulus and Density of Vacuum Casted Aluminium Alloy 2024 Containing Lithium Addition's, *Journal of Materials Engineering and Performance*, 9(3), pp. 266–271. doi: 10.1361/105994900770345908.
- McQueen, H. J. and Celliers, O. C. (1997) 'Application of Hot Workability Studies to Extrusion Processing. Part III: Physical and Mechanical Metallurgy of Al-Mg-Si and Al-Zn-Mg Alloys', *Canadian Metallurgical Quarterly*, 36(2), pp. 73–86. doi: 10.1016/S0008-4433(97)00003-7.
- Miller, W. S. *et al.* (2000) 'Recent Development in Aluminium Alloys for the Automotive Industry', *Materials Science and Engineering A*, 280(1), pp. 37–49. doi: 10.1016/S0921-5093(99)00653-X.
- Mousavi Abarghouie, S. M. R. and Seyed Reihani, S. M. (2010) 'Investigation of Friction and Wear Behaviors of 2024 Al and 2024 Al/SiCp Composite at Elevated Temperature's, *Journal of Alloys and Compounds*, 501(2), pp. 326–332. doi: 10.1016/j.jallcom.2010.04.097.
- Mu, Z. *et al.* (2005) 'Effect of the Functional Groups in Ionic Liquid Molecules on the Friction and Wear Behavior of Aluminium Alloy in Lubricated Aluminium-on-Steel Contact', *Tribology International*, 38(8), pp. 725–731. doi: 10.1016/j.triboint.2004.10.003.
- Muratoglu, M. and Aksoy, M. (2000) 'The Effects of Temperature on Wear Behaviors of Al-Cu alloy and Al-Cu/SiC Composite', *Materials Science and Engineering A*, 282(1–2), pp. 91–99. doi: 10.1016/S0921-5093(99)00767-4.
- Muratoğlu, M. and Aksoy, M. (2006) 'Abrasive Wear of 2124Al-SiC

Composites in the Temperature Range 20-200 °C', *Journal of Materials Processing Technology*, 174(1-3), pp. 272-276. doi: 10.1016/j.jmatprotec.2006.01.010.

Natarajan, S. *et al.* (2009) 'Sliding Wear Behavior of Al 6063/TiB₂ in situ Composites at Elevated Temperature's, *Materials and Design*, 30(7), pp. 2521-2531. doi: 10.1016/j.matdes.2008.09.037.

Nie, X. *et al.* (1999) 'Thickness Effects on the Mechanical Properties of Micro-Arc Discharge Oxide Coatings on Aluminium Alloy's, *Surface and Coatings Technology*, 116-119, pp. 1055-1060. doi: 10.1016/S0257-8972(99)00089-4.

Parsi, M., Najmi, K., Najafifard, F., Hassani, S., McLaury, B.S. and Shirazi, S.A., 2014. A comprehensive review of solid particle erosion modeling for oil and gas wells and pipelines applications. *Journal of Natural Gas Science and Engineering*, 21, pp.850-873.

Paulraj, P. and Harichandran, R. (2020) 'The Tribological Behavior of Hybrid Aluminium Alloy Nanocomposites at High Temperature: Role of Nanoparticle's, *Journal of Materials Research and Technology*, 9(5), pp. 11517-11530. doi: 10.1016/j.jmrt.2020.08.044.

Pauschitz, A., Roy, M. and Franek, F. (2008) 'Mechanisms of Sliding Wear of Metals and Alloys at Elevated Temperature's, *Tribology International*, 41(7), pp. 584-602. doi: 10.1016/j.triboint.2007.10.003.

Podgornik, B., 2022. Adhesive Wear Failures. *Journal of Failure Analysis and Prevention*, 22(1), pp.113-138. doi: 10.1007/s11668-021-01322-4.

Praharaj, S. (2009) 'Processing and Characterization of Fly Ash - Quartz Coating's, Department of Metallurgical and Materials Engineering National Institute of Technology Rourkela, 12(January 2009), pp. 2-3.

Qutub, A. Al *et al.* (2010) 'Elevated Temperature Wear of Submicron Al₂O₃

Reinforced 6061 Aluminium Composite’, *Advanced Materials Research*, 86, pp. 1288–1296. doi: 10.4028/www.scientific.net/AMR.83-86.1288.

Rajan, H. B. M. *et al.* (2014) ‘Effect of TiB₂ Content and Temperature on Sliding Wear Behavior of AA7075 / TiB₂ In situ Aluminium Cast Composite’s, *Archives of Civil and Mechanical Engineering*, 14(1), pp. 72–79. doi: 10.1016/j.acme.2013.05.005.

Rajaram, G. *et al.* (2010) ‘Studies on High Temperature Wear and its Mechanism of Al – Si / Graphite Composite Under Dry Sliding Condition’s, *Tribology International*, 43(11), pp. 2152–2158. doi: 10.1016/j.triboint.2010.06.004.

Rajaram, G., Kumaran, S. and Rao, T. S. (2010) ‘High Temperature Tensile and Wear Behavior of Aluminium Silicon Alloy’, *Materials Science and Engineering A*, 528(1), pp. 247–253. doi: 10.1016/j.msea.2010.09.020.

Rao, R. N. *et al.* (2009) ‘Dry Sliding Wear Behavior of Cast High Strength Aluminium Alloy (Al-Zn-Mg) and Hard Particle Composite’s, *Wear*, 267(9–10), pp. 1688–1695. doi: 10.1016/j.wear.2009.06.034.

Reddappa, H. N. *et al.* (2011) ‘Dry Sliding Friction and Wear Behavior of Aluminum/Beryl composites’, *Int. J. Appl. Eng. Res*, 2(2), pp. 976–4259.

Sagar, K. G., Suresh, P. M. and Sampathkumaran, P. (2021) ‘Addition of Beryl Content to Aluminium 2024 Alloy Influencing the Slide Wear and Friction Characteristic’s, *Journal of The Institution of Engineers (India): Series C*, 102(1), pp. 27–39. doi: 10.1007/s40032-020-00623-1.

Sherif, E.-S. M. *et al.* (2011) ‘Effects of Graphite on the Corrosion Behavior of Aluminum Graphite Composite in Sodium Chloride Solutions’, *Int. J. Electrochem. Sci*, 6, pp. 1085–

Siddesh Kumar N G, Ravindranath V M, G. S. S. S. (2014) ‘Dry Sliding Wear

Behavior of Hybrid Metal Matrix Composite's, *International Journal of Research in Engineering and Technology*, 3(3), pp. 554–558.

Singh, G., Kaur, M. and Upadhyaya, R. (2019) 'Wear and Friction Behavior of NiCrBSi Coatings at Elevated Temperature's, *Journal of Thermal Spray Technology*. doi: 10.1007/s11666-019-00876-y.

Singh, J. and Alpas, A. T. (1995) 'Elevated Temperature Wear of Al6061 and Al6061-20%Al₂O₃', *Scripta Metallurgica et Materiala*, 32(7), pp. 1099–1105. doi: 10.1016/0956-716X(94)00004-2.

Stachowiak, G.W. and Batchelor, A.W., 2013. *Engineering Tribology*. Butterworth-heinemann.

Straffelini, G. (2015) 'Wear Mechanism's, *Springer Tracts in Mechanical Engineering*, 11, pp. 85–113. doi: 10.1007/978-3-319-05894-8_4.

Sudagar, J., Venkateswarlu, K. and Lian, J. (2010) 'Dry Sliding Wear Properties of a 7075-T6 Aluminium Alloy Coated with Ni-P (h) in Different Pretreatment Condition's, *Journal of Materials Engineering and Performance*, 19(6), pp. 810–818. doi: 10.1007/s11665-009-9545-0.

Swain, B., Bhuyan, S., Behera, R., Mohapatra, S.S. and Behera, A., 2020. *Wear: A Serious Problem in Industry. Tribology In Materials And Manufacturing-Wear, Friction And LubricationIntechOpen*.

Tallian, T.E., Baile, G.H., Dalal, H. and Gustafsson, O.G., 1974. *Rolling Bearing Damage Atlas*. SKF Industries, Inc., Technology Services Center, King of Prussia, Pa.

Taskin, M., Caligulu, U. and Gur, A. K. (2008) 'Modeling Adhesive Wear Resistance of Al-Si-Mg-/SiCp PM Compacts Fabricated by Hot Pressing Process, by Means of ANN', *International Journal of Advanced Manufacturing Technology*, 37(7–8), pp. 715–721. doi: 10.1007/s00170-007-1000-5.

Totik, Y. *et al.* (2004) ‘The Effect of Homogenisation Treatment on Cold Deformations of AA 2014 and AA 6063 Alloy’s, *Journal of Materials Processing Technology*, 147(1), pp. 60–64. doi: 10.1016/j.jmatprotec.2003.10.026.

Vaira Vignesh, R. and Padmanaban, R. (2018) ‘Influence of Friction Stir Processing Parameters on the Wear Resistance of Aluminium Alloy AA5083’, *Materials Today: Proceedings*, 5(2), pp. 7437–7446. doi: 10.1016/j.matpr.2017.11.415.

Vaira Vignesh, R., Padmanaban, R. and Datta, M. (2018) ‘Influence of FSP on the Microstructure, Microhardness, Intergranular Corrosion Susceptibility and Wear Resistance of AA5083 Alloy’, *Tribology - Materials, Surfaces and Interfaces*, 12(3), pp. 157–169. doi: 10.1080/17515831.2018.1483295.

Wang, L. *et al.* (2010) ‘Effect of Temperature on the Frictional Behavior of an Aluminium Alloy Sliding against Steel during Ball-on-Disc Test’s, *Tribology International*, 43(1–2), pp. 299–306. doi: 10.1016/j.triboint.2009.06.009.

Wagner, C. and Traud, W. (2006) ‘Classic Paper in Corrosion Science and Engineering with a Perspective by F . Mansfeld * On the Interpretation of Corrosion Processes Through the Superposition of Electrochemical Partial Processes and on the Potential of Mixed Electrode’s, *Corrosion Science*, 62(10), pp. 843–855. doi: 10.5006/1.3279894.

Waterhouse, R.B., 1984. Fretting Wear. *Wear*, 100(1-3), pp.107-118. doi: 10.1016/0043-1648(84)90008-5.

Williams, J., 2005. *Engineering Tribology*. Cambridge University Press.

Williams, J. C. and Starke, E. A. (2003) ‘Progress in Structural Materials for Aerospace Systems’, *Acta Materialia*, 51(19), pp. 5775–5799. doi: 10.1016/j.actamat.2003.08.023.

- Wilson, S. and Alpas, A. T. (1996) 'Effect of Temperature on the Sliding Wear Performance of Al Alloys and Al Matrix Composite's, *Wear*, 196(1–2), pp. 270–278. doi: 10.1016/0043-1648(96)06923-2.
- Yan, L. M. *et al.* (2013) 'Static Softening Behaviors of 7055 Alloy During the Interval Time of Multi-Pass Hot Compression', *Rare Metals*, 32(3), pp. 241–246. doi: 10.1007/s12598-013-0065-6.
- Yang, W. W. *et al.* (2014) 'Fabrication and Mechanical Properties of High-Performance Aluminium Alloy', *Rare Metals*, 33(4), pp. 400–403. doi: 10.1007/s12598-014-0262-y.
- Yang, Z. R. *et al.* (2015) 'Dry Sliding Wear Performance of 7075 Al Alloy under Different Temperatures and Load Condition's, *Rare Metals*, pp. 2–7. doi: 10.1007/s12598-015-0504-7.
- Zhang, H. *et al.* (2007) 'Hot Deformation Behavior of the New Al-Mg-Si-Cu Aluminum Alloy during Compression at Elevated Temperatures', *Materials Characterization*, 58(2), pp. 168–173. doi: 10.1016/j.matchar.2006.04.012.
- Zhang, J. and Alpast, A. T. (1997) 'Transition Between Mild and Severe Wear in Aluminium Alloy's, *Acta materialia*, 45(2), pp. 513–528. doi: 10.1016/S1359-6454(96)00191-7
- Zhang, Z. H. *et al.* (2014) 'Changes of Microstructure of Different Quench Sensitivity 7,000 Aluminium Alloy After End Quenching', *Rare Metals*, 33(3), pp. 270–275. doi: 10.1007/s12598-014-0258-7.

LIST OF PUBLICATION

1. Ahmed, K. A. and Ramadan, D. O. (2022) ‘Study the Wear Characteristics of 2024 Aluminium Alloy at Different Temperatures’, *Computer Integrated Manufacturing Systems*, 28(11), pp. 1494–1506. doi: 10.24297/j.cims.2022.11.105.
2. Ahmed, K. A. and Ramadan, D. O. (XXX) ‘A Comparative Study on Dry Sliding Wear Behavior of Al2024 and Al7075 at Elevated Temperatures’ (under publication)



زانكۆی پۆلیته کنیکی ههولیر
ERBIL POLYTECHNIC UNIVERSITY

**لیکۆلینهوه له تایبته ندىهکانی داخوړانی دپارشتهی
ئهله منیۆم (AI2024, AI7075) له بارودۆخی جیاواز**

نامهیهکه

پیشکەشی ئهنجومهنی کۆلیژی تهکنیکی ئهندازیاری ههولیر کراوه له زانکۆی پۆلیته کنیکی ههولیر
وهک بهشیکى جیبهجیکردنی مهرجهکان بۆ بهدهست هینانی پروانامهی ماستهر له ئهندازیاری
میکانیک و وزه

له لایهن

کارمهند ابوبکر احمد

(بهکالۆریۆس له ئهندازیاری ساردکردنهوه ههواسازی، ۲۰۱۴)

به سهرپهرشتیاری

د. دلیر عوبید رهههزان

ههولیر- کوردستان

ئازار ۲۰۲۳

پوخته

لهم توڙينهويه ناميري پيواني داخوران (pin-on-disc) بو پلهي گهرمي بهرز ديزاين كراوه و دروست كراوه بو ليكولينهوه له تاييهتمهندي داخوران بو دارشتهي ئهلمينيومي ۲۰۲۴ و ۷۰۷۵ له بارودوخي جياواز وهك پلهي گهرمي و كيش و مهوداي خليسكان. ليكولينهوهكه لهسهر ناميري پيواني داخورانهكه ئهجامدراوه له حالهتي خليسكاني وشك و له مهوداي پلهي گهرمي ۲۵ بو ۲۲۵ پلهي سيليزي و كيشي ۳۰،۲۰،۱۰ نيوتن، لهگهله بري خليسكاني ۳۱۴۱،۲۳۵۶،۱۵۷۰ م. بو هموو تاقيكردنهوهكان خيرايب خليسكان ۲.۶ ماهر/چركه بوو به نهگوري. ئهجامي تاقيكردنهوهكان ئههميان دهرخستوه كه كاتيك پلهي گهرمي بهرزبیت داخوران زياد دهكات ، ههروهها زيادكردي كيش و مهوداي خليسكان دهبيته هوي زيادبوني داخوران. شيكردنهوي مايكروسكوپي دهردهخات كه شوينهواري داخورانهكان به شيويهكي گشتي ههلكهنده لهگهله دهركهوتني بريكي كه له داخوراني لكان. لهگهله ئهوهشدا پرؤسهي داخورانهكه له كهمهوه دهگوري بو شيواندن (تيكشكاندن) وه بهرهو داخوراني زور دهروات كاتيك پلهي گهرمي و كيش بهردهوام بن له زيادبوون. ميكانيزمي داخورانهكه ورده ورده دهگوريب بو دروست بوني درزي سههروهكه. ميكانيزمي داخوران لهسهر شيويه لابردني ماده به ئاراستهي خليسكان دهردهكهوي بههوي كاريگهري نهرم بونهوه له پلهي گهرمي بهرز. بهرههستي داخوراني دارشتهي ئهلمينيومي ۷۰۷۵ زياتره له دارشتهي ۲۰۲۴ به شيويهكي بهرچاو، ئهمهش بههوي سهختي و بههيزي دارشتهي ۷۰۷۵ بهراورد به دارشتهي ۲۰۲۴.